Factors affecting contaminant transformation by heat-activated persulfate

by

Nick Zrinyi

A thesis submitted to the Faculty of Graduate and Postdoctoral Affairs in partial fulfillment of the requirements for the degree of

Master of Applied Science

in

Environmental Engineering

Ottawa-Carleton Institute for Environmental Engineering
Carleton University
Ottawa, Ontario

Abstract

Persulfate-based *in situ* chemical oxidation (ISCO) involves the injection of persulfate ($S_2O_8^{2-}$) into the subsurface to remediate contaminated groundwater and soils. Although $S_2O_8^{2-}$ does not react with contaminants to an appreciable extent, it can be activated into stronger oxidants (*e.g.*, $SO_4^{\bullet}$ and $^{\bullet}OH$) by heat, alkaline solutions, dissolved iron and iron-containing minerals. The objective of the research described in this thesis is to explore the influence of temperature and background solutes on contaminant transformation by heat- and mineral-activated $S_2O_8^{2-}$. Through the transformation of benzoic acid (a model organic compound) and chlorendic acid (a flame retardant), it was discovered that temperature affects not only the rate of contaminant transformation but also the transformation pathway and distribution of byproducts. Solution pH, alkalinity, and chloride also influence the rates of persulfate activation and contaminant degradation. These novel understandings may help improve the design and operation of $S_2O_8^{2-}$-based remedial systems.

Table of Contents

List of Figures

List of Acronyms and Abbreviations

AC	Alternating current
ACN	Acetonitrile
BA	Benzoic acid
CA	Chlorendic acid
DC	Direct current
DF	Decarboxylation fraction
DR	Decarboxylation ratio
EDTA	Ethylenediaminetetraacetic acid
EK-TAP	Electrokinetic and thermal activation or persulfate
HBA	Hydroxybenzoic acid
HPLC	High pressure liquid chromatography
IC	Ion chromatography
ISCO	*In situ* chemical oxidation
MTBE	Methyl tert-butyl ether
NOM	Natural organic matter
PDS	Per(oxydi)sulfate
PMS	Peroxymonosulfate
TOC	Total organic carbon
UV	Ultraviolet

Preface

Chapter 3 of this thesis has been reprinted from Zrinyi, N; Pham, A.L.T. Oxidation of benzoic acid by heat-activated persulfate: effect of temperature on transformation pathway and product distribution. *Water Research* 2017, 120, 43-51. Copyright 2017 Elsevier Ltd.

Chapter 4 is a non-copyrighted manuscript.

I, Nick Zrinyi, declare that this dissertation is my original work. I was fully involved in setting up and conducting the research, obtaining data and analyzing results, as well as preparing and writing the material presented in this integrated thesis.

Dr. Anh Pham, in his capacity as Nick Zrinyi's supervisor, confirms that the assessment made by the candidate above is a valid and accurate. Dr. Anh Pham was the supervisory author and was involved with concept formation and manuscript composition.

1.0 Introduction

1.1 Motivation

It has been widely acknowledged that hazardous waste sites, created due to unregulated and improper disposal of toxic chemicals in the previous century, are among the most problematic pollution hotspots in North America. In the United States, even after significant investment in remediation efforts, the country still has over 300,000 federal and private hazardous waste sites whose clean-up will require an additional of $200 billion in the coming decades (EPA, 2004). In Canada, the Parliamentary Budget Officer in 2014 reported that there are over 22,000 federal hazardous waste sites, many of which are heavily contaminated and pose direct threats to environmental and public health (Story and Yalkin, 2014). The report also predicted that if we were to use existing technologies, such as groundwater extraction and soil excavation, to remediate these sites, approximately $4.9 billion will be needed for the clean-up (Story and Yalkin, 2014). Therefore, new technologies that improve the efficiency of site clean-up have the potential for significant economic benefits in both cost savings and the time required for site remediation.

In situ chemical oxidation (ISCO) is appealing for remediation of soil and groundwater because it is fast and cost effective. ISCO involves the injection of an oxidant into contaminated areas to initiate chemical reactions that can destroy contaminants. Common oxidants used in this practice include catalyzed hydrogen peroxide (CHP), permanganate, ozone and persulfate. While CHP and permanganate have been widely employed in the last three decades (Figure 1.1), persulfate ($S_2O_8^{2-}$) is gaining popularity

especially in the last ten years. Compared with CHP and permanganate, $S_2O_8^{2-}$ provides several advantages. First, unlike permanganate which can only oxidize a limited number of contaminants, $S_2O_8^{2-}$ is effective at destroying a wide variety of organic contaminants including chlorinated organic solvents, BTEX (*i.e.*, benzene, toluene, ethylbenzene, and xylene), polycyclic aromatic hydrocarbons (PAHs), and polychlorinated biphenyls (PCBs). This is because $S_2O_8^{2-}$ can be activated into sulfate and hydroxyl radicals ($SO_4^{\bullet-}$ and $^{\bullet}OH$, respectively), which are very powerful oxidants that can react with contaminants at near diffusion-limited rates (Buxton et al., 1988). Although CHP can also oxidize contaminants via $^{\bullet}OH$-based reactions, its utility is limited because hydrogen peroxide often disappears quickly upon injection into the subsurface. In contrast, $S_2O_8^{2-}$ is relatively stable and therefore can migrate deep into contaminated areas far away from the injection well. Additionally, the byproducts of persulfate decomposition are sulfate ions and oxygen, which are benign to the environment and do not cause subsurface clogging (the reduction of permanganate produces manganese dioxide (MnO_2) which can decrease subsurface hydraulic conductivity).

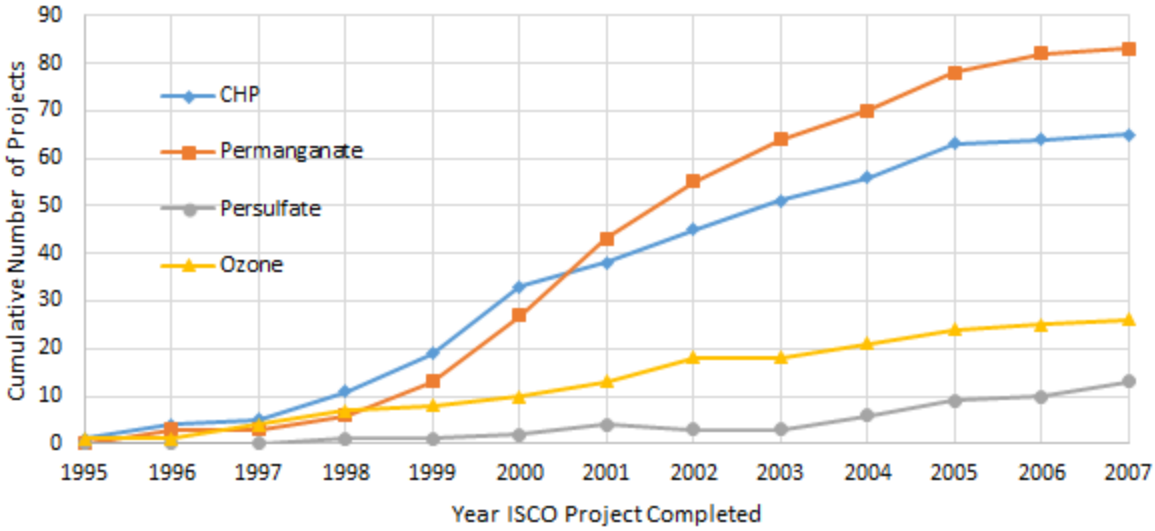

Figure 1.1: Frequency of ISCO oxidant use between 1995 and 2007 (adapted from Krembs, 2008)

$S_2O_8^{2-}$ can be activated into $SO_4^{\bullet-}$ and $^{\bullet}OH$ by heat, dissolved metals and metal oxides, and alkaline solutions. Heat can be introduced into the subsurface by steam injection, addition of H_2O_2 (the decomposition of H_2O_2 is an exothermic reaction), or via electrical resistance heating. Dissolved metals and base activations involve the injection of dissolved metals (*e.g.*, Fe(II), Co(III)) or alkaline solutions (*e.g.,* NaOH) into the subsurface together with $S_2O_8^{2-}$. $S_2O_8^{2-}$ can also be used without the addition of an activator. Although usually referred to as un-activated $S_2O_8^{2-}$, this approach relies on the ability of naturally occurring minerals such as iron and manganese oxides to convert $S_2O_8^{2-}$ into $SO_4^{\bullet-}$ and $^{\bullet}OH$. Other activators include ultraviolet light, ultrasound, gamma rays, and photocatalysts (*e.g.,* UV/TiO_2). These activators can be used for *ex situ* remediation (*i.e.*, pump-and-treat remediation), or for treatment of municipal and industrial wastewater.

In the last decade, researchers and remediation practitioners have put significant efforts into investigating the use of $S_2O_8^{2-}$ for contaminant remediation. Despite these efforts,

the mechanisms of $S_2O_8^{2-}$ activation and contaminant oxidation as well as factors affecting these processes are not fully understood. To advance our knowledge about the chemistry of $S_2O_8^{2-}$ and the utility of $S_2O_8^{2-}$ in ISCO, this Master of Applied Science research aims to address several fundamental questions regarding the mechanism of contaminant transformation in heat-activated $S_2O_8^{2-}$ systems, and the use of persulfate for the remediation of chlorendic acid, an exotic, recalcitrant contaminant. This research investigated the effect of temperature (20 - 70°C) on the oxidation of benzoic acid by $S_2O_8^{2-}$ and the formation and distribution of oxidation byproducts (Chapter 3). Benzoic acid was used as a model compound representing naphthenic acids, a group of toxic organic contaminants present at sites contaminated with oil sands process water. Another aim of this dissertation was to investigate the ability of heat-activated $S_2O_8^{2}$to destroy chlorendic acid, a toxic polychlorinated organic acid (Chapter 4). Overall, this dissertation aims to address a number of mechanistic questions, the information of which can help improve the design of heat-activated $S_2O_8^{2-}$ ISCO systems.

1.2 Background

1.2.1 Persulfate

Although $S_2O_8^{2-}$ is a strong oxidant (E° = 2.08 V) (Bard et al., 1985), it reacts with contaminants at rates that are too slow to be practical. Therefore, the use of $S_2O_8^{2-}$ in contaminant treatment applications does not rely on the direct reaction between $S_2O_8^{2-}$ and contaminants but on the ability of $S_2O_8^{2-}$ to produce $SO_4^{\bullet-}$ and $^{\bullet}OH$, the process known as $S_2O_8^{2-}$ activation. The activation of $S_2O_8^{2-}$ takes place via the following reactions:

$$S_2O_8^{2-} \rightarrow 2SO_4^{\bullet-} \quad (1.1)$$

$$SO_4^{\bullet-} + H_2O \rightarrow {}^{\bullet}OH + SO_4^{2-} + H^+ \quad (1.2)$$

$$SO_4^{\bullet-} + OH^- \rightarrow {}^{\bullet}OH + SO_4^{2-} \quad (1.3)$$

$SO_4^{\bullet-}$ and $^{\bullet}OH$ are very strong oxidants that react with many contaminants including some of the most persistent ones such as PAHs and PCBs at near diffusion-controlled rates (*i.e.*, $k \approx 10^{9\text{-}10}$ $M^{-1}s^{-1}$) (Buxton et al., 1988):

$$SO_4^{\bullet-} + contaminants \rightarrow byproducts + SO_4^{\bullet-} \rightarrow\rightarrow\rightarrow CO_2 + H_2O + SO_4^{2-} \quad (1.4)$$

$$^{\bullet}OH + contaminants \rightarrow byproducts + {}^{\bullet}OH \rightarrow\rightarrow\rightarrow CO_2 + H_2O \quad (1.5)$$

$SO_4^{\bullet-}$ and $^{\bullet}OH$ react with organic contaminants via three distinct mechanisms, namely 1) abstraction of hydrogen atoms, 2) addition to double bonds, and 3) abstraction of electrons. Whereas $^{\bullet}OH$ oxidize contaminants mainly via the first two mechanisms (Nelson, 1955), reactions with $SO_4^{\bullet-}$ proceed mainly via the latter mechanism (Buxton et al., 1988). The byproducts produced from these reactions can be further oxidized by $SO_4^{\bullet-}$ and $^{\bullet}OH$ to generate lower molecular-weight compounds that are often less toxic and more bioavailable. The lower molecular-weight compounds can also react further with $SO_4^{\bullet-}$ and $^{\bullet}OH$ to eventually become CO_2 and H_2O (*i.e.*, mineralization).

The reactions above describe the formation of reactive species and the oxidation of contaminants. However, it is noted that the chemistry of $S_2O_8^{2-}$ is extremely complex. For example, $SO_4^{\bullet-}$ and $^{\bullet}OH$ produced in reactions 1.1-1.3 can also react with $S_2O_8^{2-}$ via the following reactions:

$$SO_4^{\bullet-} + S_2O_8^{2-} \rightarrow SO_4^{2-} + S_2O_8^{\bullet-} \quad (1.6)$$

(Buxton et al., 1988)

$$^{\bullet}OH + S_2O_8^{2-} \rightarrow SO_4^{\bullet-} + \frac{1}{2}O_2 + HSO_4^- \quad (1.7)$$

(Bartlett, 1949)

Although it has been speculated that the persulfate radical ($S_2O_8^{\bullet-}$) can also oxidize organic contaminants, its reactivity is currently not well understood. $SO_4^{\bullet-}$ and $^{\bullet}OH$ can also participate in many reactions with background electrolytes (e.g., OH^-, Cl^-, HCO_3^-, natural organic matter) that can either propagate or terminate the formation of radicals (will be discussed further in section 1.3.3). Also, while both $SO_4^{\bullet-}$ and $^{\bullet}OH$ are produced from $S_2O_8^{2-}$ activation, the relative importance of these radicals towards contaminant oxidation depends on the solution chemistry and activation method. For example, $^{\bullet}OH$ is the predominant oxidant when $S_2O_8^{2-}$ is activated by alkaline solutions or by Fe-EDTA. In contrast, $SO_4^{\bullet-}$ is the predominant oxidant when $S_2O_8^{2-}$ is activated by heat and UV/light at neutral and acidic pH. Due to this complexity, it is extremely difficult to predict the rate at which persulfate is consumed, the yield of $SO_4^{\bullet-}$ and $^{\bullet}OH$, the rate and mechanism of contaminant transformation, and the nature of the byproducts produced.

1.2.2 Methods of Persulfate Activation

As mentioned above, $S_2O_8^{2-}$ can be activated by several methods. The objective of this section is to further describe the activation of $S_2O_8^{2-}$ by heat, alkaline solutions, and dissolved iron as these activation methods are the most frequently used in *in situ* remediation. This section will also discuss some of the factors that affect the transformation of contaminants in persulfate-based ISCO, and identify knowledge gaps to be addressed in this dissertation.

1.2.2.1 Activation by Heat

$S_2O_8^{2-}$ solution is relatively stable at room temperature. At elevated temperatures, $S_2O_8^{2-}$ is decomposed into sulfate ions (SO_4^{2-}) and oxygen (O_2) according to the following reactions:

$$S_2O_8^{2-} + heat \rightarrow 2SO_4^{\bullet-} \quad (1.8)$$

$$SO_4^{\bullet-} + H_2O \rightarrow SO_4^{2-} + {}^{\bullet}OH + H^+ \quad (1.9)$$

$$SO_4^{\bullet-} + OH^- \rightarrow SO_4^{2-} + {}^{\bullet}OH \quad (1.10)$$

$$2{}^{\bullet}OH \rightarrow H_2O_2 \quad (1.11)$$

$$H_2O_2 \rightarrow H_2O + O_2 \quad (1.12)$$

Overall reaction: $$2S_2O_8^{2-} + 2H_2O \rightarrow 4SO_4^{2-} + O_2 + 4H^+ \quad (1.13)$$

In the presence of an organic contaminant, $SO_4^{\bullet-}$ generated in reaction 1.8 will react with contaminants according to the following reaction:

$$SO_4^{\bullet-} + contaminant \rightarrow products \quad (1.14)$$

The branching between reactions 1.9, 1.10 and 1.14 is controlled by the concentration of the contaminant and its reactivity with $SO_4^{\bullet-}$. Under acidic and neutral pH, reactions 1.9 and 1.10 are very slow. Therefore, the transformation of contaminants is mainly attributable to the reaction with $SO_4^{\bullet-}$ (reaction 1.14). At alkaline pH, the contribution of ${}^{\bullet}OH$ to contaminant oxidation (reaction 1.5) could be significant because $SO_4^{\bullet-}$ can be quickly converted into ${}^{\bullet}OH$ via reaction 1.10. Therefore, depending on the pH at which $S_2O_8^{2-}$ is activated, either $SO_4^{\bullet-}$, ${}^{\bullet}OH$, or both radicals can contribute to the oxidation of contaminant. For example, Dogliotti and Hayon (1967) pointed out that conversion of $SO_4^{\bullet-}$ to ${}^{\bullet}OH$ is significantly enhanced above pH 8.5. More recently, it was also

demonstrated that $SO_4^{\bullet-}$ was the dominant radical species below pH 7, both $SO_4^{\bullet-}$ and $^{\bullet}OH$ were present at pH 9, and $^{\bullet}OH$ was dominant at pH 12 (Liang and Su, 2009).

The rates of $S_2O_8^{2-}$ decomposition and reactive radical generation depend on the solution temperature. The half-life of persulfate decomposition ranges from 4.8 months to 8.6 hours at 30°C and 70°C, respectively (Johnson et al., 2008). As a result, increasing solution temperature will accelerate the production of $SO_4^{\bullet-}$ and $^{\bullet}OH$ and therefore speed up contaminant oxidation. For example, it has been shown that contaminants such as chlorinated solvents (Waldemer et al., 2007), petroleum hydrocarbons (Huang et al., 2005), herbicides (Ji et al., 2015a; Tan et al., 2012; Romero et al., 2010), and pharmaceuticals (Ghauch et al., 2012; Ghauch and Tuqan, 2012; Tan et al., 2013; Oncu et al., 2015; Ji et al., 2015b) can be completely destroyed within a few hours with $S_2O_8^{2-}$ that was activated at 40-70°C.

While most studies looked at the effect of temperature on the rates of $S_2O_8^{2-}$ activation and contaminant transformation, a few studies suggest that temperature may have other effects beyond controlling reaction rates. For example, a study found that higher activation temperatures produced a greater fraction of toxic brominated and iodinated disinfection byproducts (Chu et al., 2016). Another study by Mora et al. (2011) showed that phenol transformation by activated $S_2O_8^{2-}$ occurred via polymerization at higher temperatures and hydroxylation at lower temperatures (Mora et al., 2011). ***These results suggest that temperature may control the pathway through which contaminants are transformed by heat-activated $S_2O_8^{2-}$, a phenomenon that merits further investigation.***

Methods to thermally activate $S_2O_8^{2-}$ *in situ* include injection of steam, co-injection of H_2O_2, and applying either DC or AC current to induce electrical resistance heating. The injection of steam into the subsurface has been widely employed to extract volatile organic compounds (VOCs) from the subsurface. This technology, also known as *in situ* remediation by vapour extraction, relies on the increased volatility of the compound of interest at high temperature to strip it from the liquid phase to the gas phase, and extract it (e.g., by a vacuum pump) out of the subsurface. The technology is relatively mature and can be readily employed to activate $S_2O_8^{2-}$ once $S_2O_8^{2-}$ is delivered into the subsurface. Heat can also be introduced *in situ* by addition of H_2O_2. Remediation practitioners who injected H_2O_2 together with $S_2O_8^{2-}$ observed that the rate at which $S_2O_8^{2-}$ is activated was significantly increased in the presence of H_2O_2 (Crimi and Taylor, 2007). It was speculated that the reaction between H_2O_2 and $S_2O_8^{2-}$ resulted in the activation of the latter. However, the most plausible explanation for the role of H_2O_2 is that the decomposition of H_2O_2 by iron- and manganese-containing minerals liberates heat, which results in the activation of $S_2O_8^{2-}$ (Waldemer et al., 2007; Huling and Pivetz, 2007). Another benefit of adding H_2O_2 is that the decomposition of H_2O_2 produces O_2 bubbles, which could enhance mixing in the subsurface and therefore decrease mass transport limitation. Thermal activation of $S_2O_8^{2-}$ by electrical resistance heating involves passing direct (DC) or alternating (AC) current between the areas of interest. When employed in $S_2O_8^{2-}$-based ISCO DC can be used to migrate $S_2O_8^{2-}$, a negatively charged ion, from cathode to anode thereby enhancing the distribution of $S_2O_8^{2-}$ in the subsurface. Once the $S_2O_8^{2-}$ has been

delivered to the target contaminated area, DC is switched to AC to heat the subsurface up and activate $S_2O_8^{2-}$.

1.2.2.2 Activation by Base

At basic pH, $S_2O_8^{2-}$ is decomposed via the following reactions:

$$S_2O_8^{2-} + H_2O + OH^- \rightarrow SO_4^{2-} + HSO_5^{2-} + 2H^+ \quad (1.15)$$

$$HSO_5^{2-} + H_2O + OH^- \rightarrow SO_4^{2-} + HO_2^- + H^+ \quad (1.16)$$

$$HO_2^- + S_2O_8^{2-} \rightarrow SO_4^{\bullet-} + SO_4^{2-} + H^+ + O_2^{\bullet-} \quad (1.17)$$

Therefore, increasing solution pH will accelerate the rates of $S_2O_8^{2-}$ decomposition via reactions 1.15 and 1.16, and the generation of $SO_4^{\bullet-}$ via reaction 1.17. The $SO_4^{\bullet-}$ radical produced in reaction 1.17 can further react with contaminants (reaction 1.14), or react with hydroxide (Hayon et al., 1972):

$$SO_4^{\bullet-} + OH^- \rightarrow SO_4^{2-} + {}^{\bullet}OH \qquad k = 6.5 \times 10^7\ M^{-1}s^{-1} \quad (1.18)$$

As pH increases reaction kinetics for the conversion of $SO_4^{\bullet-}$ to $^{\bullet}OH$ (reaction 1.15) become more favourable than competing reactions, *e.g.*, the reaction between $SO_4^{\bullet-}$ and a given contaminant (reaction 1.14). For example, at pH 12 the product of hydroxide ion concentration, $[OH^-] = 10^{-2}$ M, and reaction rate constant, $k_{18} = 6.5 \times 10^7\ M^{-1}s^{-1}$ gives an observed reaction rate of $6.5 \times 10^5\ s^{-1}$. Meanwhile, assuming a typical contaminant concentration of 10 μM and reaction rate constant with $SO_4^{\bullet-}$ of $k = 10^9\ M^{-1}s^{-1}$, the observed reaction rate between the contaminant and $SO_4^{\bullet-}$ would be $10^9\ M^{-1}s^{-1} \times 10^{-5}$ M $= 10^4\ s^{-1}$. Thus, reaction 1.18 will be the predominant pathway through which $SO_4^{\bullet-}$ is consumed. This reaction produces $^{\bullet}OH$, which in turn will oxidize contaminants via reaction 1.5. Consistent with this analysis, studies have observed that $^{\bullet}OH$ is the

dominant radical species responsible for contaminant oxidation at pH 11 and above (Liang and Su, 2009; Norman et al., 1970; Dogliotti and Hayon, 1967).

The activation of persulfate by base *in situ* is realized by co-injecting a strong base (*e.g.*, NaOH or KOH). While this is a widely used remediation approach, raising solution pH could be challenging in a subsurface with high natural buffering capacity. Raising the solution pH can also exacerbate the scavenging of $SO_4^{\bullet-}$ and $^{\bullet}OH$ by carbonate ion (CO_3^{2-}), thereby decreasing the radical availability for reacting with contaminants (discussed further in section 1.3.3).

1.2.2.3 Activation by Dissolved Iron

Dissolved iron(II) reacts with persulfate via a single-electron transfer process that produces $SO_4^{\bullet-}$ and iron(III):

$$S_2O_8^{2-} + Fe^{2+} \rightarrow SO_4^{\bullet-} + Fe^{3+} + SO_4^{2-} \quad (1.19)$$

(Kolthoff et al., 1951)

The Fe^{3+} ion produced in the above reaction can be reduced back to Fe^{2+} via reaction with another persulfate molecule:

$$Fe^{3+} + S_2O_8^{2-} \rightarrow S_2O_8^{\bullet-} + Fe^{2+} \quad (1.20)$$

(Liu et al., 2016)

The cycling between Fe^{2+} and Fe^{3+} helps sustain the decomposition of persulfate and generation of $SO_4^{\bullet-}$. However, the iron redox cycling can be disrupted if Fe^{3+} precipitates out of the solution. While iron precipitates can also activate persulfate, their reactivity is much lower than that of dissolved iron. The solubility of Fe can be enhanced by adding a chelating agent such as Ethylenediaminetetraacetic acid (EDTA) or citric acid (Stumm and

Morgan, 1996). The chelating agent helps to retain iron in the solution by forming dissolved complexes:

$$[Fe(H_2O)_6]^{3+}{}_{(aq)} + EDTA^{4-}{}_{(aq)} \rightarrow [Fe(EDTA)]^{-}{}_{(aq)} + 6H_2O \quad (1.21)$$

In addition to enhancing the solubility of iron, chelating agents can have other effects on the chemistry of iron and persulfate, and the degradation of contaminants. For example, while the reaction between Fe^{2+} and persulfate produces $SO_4^{\bullet-}$ (reaction 1.19), the reaction between Fe-EDTA and persulfate produces $^{\bullet}OH$ (Liang et al., 2009). Compared with Fe^{3+}, Fe-EDTA also reacts with persulfate at a much faster rate. Additionally, EDTA is an organic molecule that can react with both $^{\bullet}OH$ and $SO_4^{\bullet-}$. Therefore, addition of excess amount of EDTA should be avoided to prevent EDTA outcompeting the contaminant for the reactive radical species.

1.3.3 Effect of Background Solutes on Contaminant Oxidation by $^{\bullet}OH$ and $SO_4^{\bullet-}$

As discussed above, soil and groundwater contain a variety of constituents (*e.g.*, OH^-, iron- and manganese-containing minerals) that may contribute to the activation of persulfate. At the same time, there are constituents that can react with $^{\bullet}OH$ and $SO_4^{\bullet-}$, thereby decreasing radical availability for contaminant oxidation. Whether the contaminant can outcompete background solutes for $^{\bullet}OH$ and $SO_4^{\bullet-}$ is determined by the concentration of each species in the solution and their reactivity with the reactive radical species. For example, bicarbonate (HCO_3^-), which is ubiquitous in groundwater, reacts with $SO_4^{\bullet-}$ very slowly:

$$SO_4^{\bullet-} + HCO_3^- \rightarrow SO_4^{2-} + HCO_3^{\bullet} \qquad k = 1.6 \times 10^6\ M^{-1}s^{-1} \quad (1.22)$$

However, the concentration of HCO_3^- in groundwater is typically orders of magnitude greater than that of a contaminant (*e.g.*, 0.01 M HCO_3^- vs 10^{-5} M contaminant). Assuming that the reaction rate between the contaminant and $SO_4^{\bullet-}$ is k = 10^9 $M^{-1}s^{-1}$, the observed rate of the reaction between the contaminant and $SO_4^{\bullet-}$ would be 10^9 $M^{-1}s^{-1}$ x 10^{-5} M = 10^4 s^{-1}. Similarly, the observed rate of reaction 1.22 would be 1.6 x 10^6 $M^{-1}s^{-1}$ x 0.01 M = 1.6 x 10^4 s^{-1}. The observed rate values indicate that at least 50% of the $SO_4^{\bullet-}$ produced from the activation of persulfate would react with bicarbonate instead of with the contaminant. As such, the rate of contaminant transformation observed in the presence of bicarbonate will be significantly slower than that observed in the absence of bicarbonate. Note that the effect of carbonate species (*i.e.*, H_2CO_3, HCO_3^-, and CO_3^{2-}) is dependent on the pH of solution. When persulfate is activated by base, the predominant carbonate species at pH > 12 would be CO_3^{2-}:

$$HCO_3^- \leftrightarrow CO_3^{2-} + H^+ \qquad pKa_2 = 10.3 \qquad (1.23)$$

The scavenging of $^{\bullet}OH$ by carbonate would be more pronounced because CO_3^{2-} is much more reactive with $^{\bullet}OH$:

$$^{\bullet}OH + HCO_3^- \rightarrow OH^- + HCO_3^{\bullet} \qquad k = 8.5 \times 10^6\ M^{-1}s^{-1} \qquad (1.24)$$
(Buxton and Elliot, 1986)

$$^{\bullet}OH + CO_3^{2-} \rightarrow OH^- + CO_3^{\bullet-} \qquad k = 4.2 \times 10^8\ M^{-1}s^{-1} \qquad (1.25)$$
(Weeks and Rabani, 1966)

In contrast, when persulfate is activated by heat, Fe-EDTA, or naturally-occurring minerals, the solution pH usually drop quickly to pH < 5 because the decomposition of

persulfate generates H^+ (reaction 1.13). The predominant carbonate species at this pH is H_2CO_3:

$$H_2CO_3 \leftrightarrow HCO_3^- + H^+ \qquad pKa_1 = 6.4 \qquad (1.26)$$

Since H_2CO_3 does not react with $^{\bullet}OH$ and $SO_4^{\bullet-}$ to an appreciable extent ($k < 10^5\ M^{-1}s^{-1}$), the effect of carbonate on the rate of contaminant oxidation would be minimal at this pH.

In addition to carbonate species, the solutes in groundwater that can compete with a contaminant for $SO_4^{\bullet-}$ include chloride, dissolved metals, natural organic matter (NOM) and others.

$$SO_4^{\bullet-} + Cl^- \rightarrow SO_4^{2-} + Cl^{\bullet} \qquad k = 2.6 \times 10^8\ M^{-1}s^{-1} \qquad (1.27)$$
(Padmaja et al., 1993)

$$SO_4^{\bullet-} + NOM \rightarrow products \qquad k = 10^6 - 10^7\ M_C^{-1}s^{-1} \qquad (1.28)$$
(Ahn et al., 2017)

$$SO_4^{\bullet-} + Fe^{2+} \rightarrow Fe^{3+} + SO_4^{2-} \qquad k = 9.9 \times 10^8\ M^{-1}s^{-1} \qquad (1.29)$$
(Neta et al., 1988)

Taking into account the competition for $SO_4^{\bullet-}$ from all solutes present in groundwater, the fraction of $SO_4^{\bullet-}$ available for reacting with the contaminant of interest can be as little as 1% of the amount produced from $S_2O_8^{2-}$ activation. Therefore, it is important to evaluate the effects of the soil and groundwater matrix on $S_2O_8^{2-}$ consumption and contaminant transformation when designing a remediation system. These effects can be investigated by conducting treatability tests in the laboratory, which help estimate the persistence of $S_2O_8^{2-}$ in the subsurface, the amount of persulfate required, and the rate of contaminant transformation.

It is noted that although NOM and Cl^- can react with $SO_4^{\bullet-}$, the effect of these solutes on the chemistry of $S_2O_8^{2-}$ is rather complex. In particular, a recent study reported that organic matter, specifically the phenol and quinone moieties in the organic matter, can also activate $S_2O_8^{2-}$ (Fang et al., 2013; Ahmad et al., 2013). The activation is described by the reactions below:

$$Q + H_2Q \rightarrow 2SQ^{\bullet-} + 2H^+ \quad (1.30)$$

$$SQ^{\bullet-} + {S_2O_8}^{2-} \rightarrow Q + {SO_4}^{\bullet-} \quad (1.31)$$

(Fang et al., 2013)

$$PhO^- + {S_2O_8}^{2-} \rightarrow {SO_4}^{2-} + {SO_4}^{\bullet-} + PhO_{ox} \quad (1.32)$$

(Ahmad et al., 2013)

n.b. where Q, SQ, and Ph, represent quinone, semiquinone, and phenol moieties respectively, and PhO_{ox} are oxidized phenol products

Therefore, on one hand NOM can compete with contaminants for $SO_4^{\bullet-}$, thereby decreasing the rate at which contaminants are transformed. On the other hand, NOM can accelerate the rate of $SO_4^{\bullet-}$ production by serving as a $S_2O_8^{2-}$ activator. Another effect of NOM on the persulfate-based ISCO is that the reaction between NOM and persulfate will accelerate the consumption of $S_2O_8^{2-}$, decreasing its longevity in the subsurface.

Regarding chloride, the reaction between $SO_4^{\bullet-}$ and Cl^- produces $Cl^{\bullet}$, which is then involved in a series of reactions that can produce either $^{\bullet}OH$ or ClO_3^-:

$${SO_4}^{\bullet-} + Cl^- \rightarrow {SO_4}^{2-} + Cl^{\bullet} \quad \text{(Padmaja et al., 1993)} \quad (1.33)$$

$$Cl^{\bullet} + H_2O \rightarrow HOCl^{\bullet-} + H^+ \quad \text{(Buxton et al., 1998)} \quad (1.34)$$

$$HOCl^{\bullet-} + H_2O \rightarrow OH^{\bullet} + Cl^- \quad \text{(Jayson et al., 1973)} \quad (1.35)$$

$$Cl^{\bullet} + Cl^- \leftrightarrow {Cl_2}^{\bullet-} \quad \text{(Nagarajan and Fessenden, 1985)} \quad (1.36)$$

$Cl_2^{\bullet-} + Cl_2^{\bullet-} \rightarrow Cl_2 + 2Cl^-$ (Yu et al., 2004) (1.37)

$Cl_2 + H_2O \rightarrow HOCl + Cl^- + H^+$ (Lifshitz and Perlmutter-Hayman, 1960) (1.38)

$HOCl \leftrightarrow H^+ + ClO^-$ (Haag and Hoigne, 1983) (1.39)

$ClO^- + OH^\bullet \rightarrow ClO^\bullet + OH^-$ (Buxton and Subhani, 1972) (1.40)

$2ClO^\bullet + H_2O \rightarrow ClO^- + {ClO_2}^- + 2H^+$ (Kläning and Wolff, 1985) (1.41)

${ClO_2}^- + OH^\bullet \rightarrow {ClO_2}^\bullet + OH^-$ (Kläning et al., 1985) (1.42)

${ClO_2}^\bullet + OH^\bullet \rightarrow {ClO_3}^- + H^+$ (Kläning et al., 1985) (1.43)

The reaction between $SO_4^{\bullet-}$ and Cl^- at neutral pH produces $^\bullet OH$. Therefore, Cl^- is not considered to be a competing solute because the reaction produces another strong oxidant that can react with contaminants. At pH < 5, Cl^- is considered as a radical scavenger (*i.e.*, competing solute) because the reaction did not produce a secondary radical that can be used to oxidize contaminants. Moreover, the reaction at this pH produces ClO_3^-, a potentially toxic compound. In $S_2O_8^{2-}$-based ISCO (except base-activated $S_2O_8^{2-}$), the pH of groundwater can drop quickly to as low as pH < 3 upon addition of $S_2O_8^{2-}$ because the decomposition of persulfate produces H^+. As such, the effect of Cl^- on the kinetics of contaminant transformation and the production of ClO_3^- when pH drops to below 5 should be considered when designing and operating persulfate-based ISCO remediation systems. ***As will be discussed in chapter 4, the effect of Cl^- is particularly relevant to the remediation of chlorendic acid.***

1.2 Organization of Subsequent Chapters

The overall objective of this dissertation is to gain better insights into factors affecting the efficiency of contaminant oxidation by heat- and mineral-activated persulfate. **Chapter 2** describes the materials, experimental design, and analytical techniques employed in

subsequent chapters. **Chapter 3**, entitled “Oxidation of benzoic acid by heat-activated persulfate: Effect of temperature on transformation pathway and product distribution”, is a paper that was published in *Water Research* on April 28, 2017. This paper used benzoic acid as a model compound to examine the effect of temperature on the transformation mechanism, formation of byproducts, and $S_2O_8^{2-}$ utilization efficiency. **Chapter 4**, entitled “Mechanistic study of chlorendic acid removal by heat-activated persulfate”, is a manuscript that is under preparation for a journal publication. This chapter assesses heat- and mineral-activated persulfate as means of destroying chlorendic acid, which is a toxic organo-chloride flame retardant whose fate and transformation has not been thoroughly investigated. The ability of persulfate to destroy chlorendic acid was investigated in synthetic solutions prepared in the laboratory. The last chapter, **Chapter 5**, summarizes key findings and discusses future research directions. A list of references is provided at the end of each chapter.

1.3 References

Ahmad, M., A. L. Teel, and R. J. Watts. "Mechanism of Persulfate Activation by Phenols." *Environmental Science & Technology* 47.11 (2013): 5864-871.

Ahn, Y., D. Lee, M. Kwon, I. Choi, S. Nam, and J. Kang. "Characteristics and Fate of Natural Organic Matter during UV Oxidation Processes." *Chemosphere* 184 (2017): 960-68.

Bard, A. J., R. Parsons, and J. Jordan. *Standard Potentials in Aqueous Solution*. Boca Raton: CRC in Imprint of the Taylor & Francis Group, 1985.

Bartlett, P.D., J. D. Cotman. “The Kinetics and Decomposition or Potassium Persulfate in Aqueous Solutions of Methanol.” *Journal of the American Chemical Society*. 71.4 (1949): 1419-22.

Buxton, G. V., and M. S. Subhani. "Radiation Chemistry and Photochemistry of Oxychlorine Ions. Part 2.—Photodecomposition of Aqueous Solutions of Hypochlorite Ions." *Journal of the Chemical Society, Faraday Transactions 1: Physical Chemistry in Condensed Phases* 68.0 (1972): 958.

Buxton, G. V., C. L. Greenstock, W. Phillips Helman, and Alberta B. Ross. "Critical Review of Rate Constants for Reactions of Hydrated Electrons, Hydrogen Atoms and Hydroxyl Radicals (•OH/•O− in Aqueous Solution." *Journal of Physical and Chemical Reference Data* 17.2 (1988): 513-886.

Buxton, G. V., and A. J. Elliot. "Rate Constant for Reaction of Hydroxyl Radicals with Bicarbonate Ions." International Journal of Radiation Applications and Instrumentation. Part C. *Radiation Physics and Chemistry* 27.3 (1986): 241-43

Buxton, G. V., M. Bydder, and G. A. Salmon. "Reactivity of Chlorine Atoms in Aqueous Solution: Part 1 The Equilibrium $Cl^{\bullet}$ <-> Cl^- + $Cl_2^{\bullet-}$." *Journal of the Chemical Society, Faraday Transactions* 94.5 (1998): 653-57.

Chu, W., J. Hu, T. Bond, N. Gao, B. Xu, and D. Yin. "Water Temperature Significantly Impacts the Formation of Iodinated Haloacetamides during Persulfate Oxidation." *Water Research* 98 (2016): 47-55.

Crimi, M. L. and Taylor, J. 2007. “Experimental Evaluation of Catalyzed Hydrogen Peroxide and Sodium Persulfate for Destruction of BTEX Contaminants.” *Soil & Sediment Contamination*, 16: 29–45.

Dogliotti, L., and E. Hayon. "Flash Photolysis of Per[oxydi]sulfate Ions in Aqueous Solutions. The Sulfate and Ozonide Radical Anions." *The Journal of Physical Chemistry* 71.8 (1967): 2511-516.

EPA. “Cleaning up the Nation's Waste Sites: Markets and Technology Trends”. Washington, DC: U.S. Environmental Protection Agency, Office of Solid Waste and Emergency Response, Washington, D.C. 2004.

Huling, S.G. and B. Pivetz. In-Situ Chemical Oxidation -- Engineering Issue. EPA/600/R-06/072, 2007.

Fang, G., Juan G., D. D. Dionysiou, C. Liu, and D. Zhou. "Activation of Persulfate by Quinones: Free Radical Reactions and Implication for the Degradation of PCBs." *Environmental Science & Technology* 47.9 (2013): 4605-611.

Ghauch, Antoine, A., and N. Kibbi. "Ibuprofen Removal by Heated Persulfate in Aqueous Solution: A Kinetics Study." *Chemical Engineering Journal* 197 (2012): 483-92.

Ghauch, A., and A. Tuqan. "Oxidation of Bisoprolol in Heated Persulfate/H_2O Systems: Kinetics and Products." *Chemical Engineering Journal* 183 (2012): 162-71.

Haag, W. R., and J. Hoigné. "Ozonation of Water Containing Chlorine or Chloramines. Reaction Products and Kinetics." *Water Research* 17.10 (1983): 1397-402.

Hayon, E., A. Treinin, and J. Wilf. "Electronic Spectra, Photochemistry, and Autoxidation Mechanism of the Sulfite-bisulfite-pyrosulfite Systems. SO_2^-, SO_3^-, SO_4^-, and SO_5^- Radicals." *Journal of the American Chemical Society* 94.1 (1972): 47-57.

Huang, K., Z. Zhao, G. E. Hoag, A. Dahmani, and P. A. Block. "Degradation of Volatile Organic Compounds with Thermally Activated Persulfate Oxidation." *Chemosphere* 61.4 (2005): 551-60.

Jayson, G. G., B. J. Parsons, and A. J. Swallow. "Some Simple, Highly Reactive, Inorganic Chlorine Derivatives in Aqueous Solution. Their Formation Using Pulses of Radiation and Their Role in the Mechanism of the Fricke Dosimeter." *Journal of the Chemical Society, Faraday Transactions 1: Physical Chemistry in Condensed Phases* 69.0 (1973): 1597.

Ji, Y., C. Dong, D. Kong, J. Lu, and Q. Zhou. "Heat-activated Persulfate Oxidation of Atrazine: Implications for Remediation of Groundwater Contaminated by Herbicides." *Chemical Engineering Journal* 263 (2015): 45-54.

Ji, Y., Y. Fan, K. Liu, D. Kong, and J. Lu. "Thermo Activated Persulfate Oxidation of Antibiotic Sulfamethoxazole and Structurally Related Compounds." *Water Research* 87 (2015): 1-9.

Johnson, R. L., P. G. Tratnyek, and Reid O'Brien Johnson. "Persulfate Persistence under Thermal Activation Conditions." *Environmental Science & Technology* 42.24 (2008): 9350-356.

Kläning, U. K., K. Sehested, and J. Holcman. " Standard Gibbs Energy of Formation of the Hydroxyl Radical in Aqueous Solution. Rate Constants for the Reaction ClO_2^- + O_3^- ↔ O_3 + ClO_2." *Chemischer Informationsdienst* 16.23 (1985).

Kläning, U. K., and T. Wolff. "Laser Flash Photolysis of HClO, ClO^-, HBrO, and BrO^- in Aqueous Solution. Reactions of Cl^- and Br^- Atoms." *Berichte Der Bunsengesellschaft Für Physikalische Chemie* 89.3 (1985): 243-45.

Kolthoff, I. M., A. I. Medalia, and H. Parks Raaen. "The Reaction between Ferrous Iron and Peroxides. IV. Reaction with Potassium Persulfate." *Journal of the American Chemical Society* 73.4 (1951): 1733-739.

Krembs FJ. 2008. Critical Analysis of the Field Scale Application of *In Situ* Chemical Oxidation for the Remediation of Contaminated Groundwater. MS Thesis. Colorado School of Mines Department of Environmental Science and Engineering, Golden, CO, USA. April.

Liang, C., and H. Su. "Identification of Sulfate and Hydroxyl Radicals in Thermally Activated Persulfate." *Industrial & Engineering Chemistry Research* 48.11 (2009): 5558-562.

Liang, C., C. Liang, and C. Chen. "PH Dependence of Persulfate Activation by EDTA/Fe(III) for Degradation of Trichloroethylene." *Journal of Contaminant Hydrology* 106.3-4 (2009): 173-82.

Lifshitz, A., and B. Perlmutter-Hayman. "The Kinetics of The Hydrolysis Of Chlorine. I. Reinvestigation of The Hydrolysis In Pure Water." *The Journal of Physical Chemistry* 64.11 (1960): 1663-665.

Liu, H., T. A. Bruton, W. Li, J. Van Buren, C. Prasse, F. M. Doyle, and D. L. Sedlak. "Oxidation of Benzene by Persulfate in the Presence of Fe(III)- and Mn(IV)-Containing Oxides: Stoichiometric Efficiency and Transformation Products." *Environmental Science & Technology* 50.2 (2016): 890-98.

Lutze, H. V., N. Kerlin, and T. C. Schmidt. "Sulfate Radical-based Water Treatment in Presence of Chloride: Formation of Chlorate, Inter-conversion of Sulfate Radicals into Hydroxyl Radicals and Influence of Bicarbonate." *Water Research* 72 (2015): 349-60.

Mora, V. C., J. A. Rosso, Daniel O. Mártire, and Mónica C. Gonzalez. "Phenol Depletion by Thermally Activated Peroxydisulfate at 70°C." *Chemosphere* 84.9 (2011): 1270-275.

Nagarajan, V., and R. W. Fessenden. "Flash Photolysis of Transient Radicals: 1. X_2^- with X = Cl, Br, I, and SCN." *The Journal of Physical Chemistry* 89.11 (1985): 2330-335.

Nelson, Peter F. "Aromatic Substitution by Free Radicals." *Journal of Chemical Education* 32.12 (1955): 606.

Neta, P., Huie, R.E., Ross, A.B. Rate Constants for Reactions for Inorganic Radicals in Aqueous Solution. *Journal of Physical and Chemical Reference Data* (1988): 17, 1027–1247.

Norman, R. O. C., P. M. Storey, and P. R. West. "Electron Spin Resonance Studies. Part XXV. Reactions of the Sulphate Radical Anion with Organic Compounds." *Journal of the Chemical Society B: Physical Organic* (1970): 1087.

Oncu, N. Bilgin, N. Mercan, and I. A. Balcioglu. "The Impact of Ferrous Iron/heat-activated Persulfate Treatment on Waste Sewage Sludge Constituents and Sorbed Antimicrobial Micropollutants." *Chemical Engineering Journal* 259 (2015): 972-80.

Padmaja, S., P. Neta, and R. E. Huie. "Rate Constants for Some Reactions of Inorganic Radicals with Inorganic Ions. Temperature and Solvent Dependence." *International Journal of Chemical Kinetics* 25.6 (1993): 445-55.

Story, R., T. Yalkin. “Federal Contaminated Sites Cost”. Office of the Parliamentary Budget Officer. Ottawa, Canada, 2014

Romero, A., A. Santos, F. Vicente, and Concepción González. "Diuron Abatement Using Activated Persulphate: Effect of PH, Fe(II) and Oxidant Dosage." *Chemical Engineering Journal* 162.1 (2010): 257-65.

Stumm, W., J. J. Morgan. *Aquatic Chemistry: Chemical Equilibria and Rates in Natural Waters*. New York: Wiley, 1996.

Tan, C., N. Gao, Y.Deng, W. Rong, S. Zhou, and N. Lu. "Degradation of Antipyrine by Heat Activated Persulfate." *Separation and Purification Technology* 109 (2013): 122-28.

Tan, C., N. Gao, Y. Deng, N. An, and J. Deng. "Heat-activated Persulfate Oxidation of Diuron in Water." *Chemical Engineering Journal* 203 (2012): 294-300.

Waldemer, R. H., P. G. Tratnyek, R. L. Johnson, and J. T. Nurmi. "Oxidation of Chlorinated Ethenes by Heat-Activated Persulfate: Kinetics and Products." *Environmental Science & Technology* 41.3 (2007): 1010-015.

Weeks, J. L., and J. Rabani. "The Pulse Radiolysis of Deaerated Aqueous Carbonate Solutions. I. Transient Optical Spectrum and Mechanism. II. PK for OH Radicals." *The Journal of Physical Chemistry* 70.7 (1966): 2100-106.

Yu, X., Z. Bao, and J. R. Barker. "Free Radical Reactions Involving $Cl^{\bullet}$, and $Cl_2^{\bullet-}$, and $SO_4^{\bullet}$ in the 248 nm Photolysis of Aqueous Solutions Containing $S_2O_8^{2-}$ and Cl^-." *ChemInform* 35.14 (2004): 295-308.

2.0 Materials and Methods

2.1 Chemicals

All chemicals were of ACS reagent grade and were used without further purification. Benzoic acid, potassium persulfate, potassium iodide, potassium phosphate, and sodium bicarbonate were obtained from VWR International. Chlorendic acid, methyl tert-butyl ether (MTBE), sodium persulfate and other organic compounds (o, m, p-hydroxybenzoic acids, phenol, catechol, hydroquinone, 4-nitrobenzoic acid) were obtained from Sigma-Aldrich. All solutions were prepared using 18.2 MΩ·cm water (Millipore System).

2.2 Experimental Setup

Persulfate activation and benzoic acid (BA) oxidation experiments were conducted in 16 mL sealed test tubes that contained 10 mL of reaction solution. The initial concentrations of BA and persulfate were 0.1 – 5 mM and 1 mM, respectively. In remediation practice, the concentration of persulfate is usually much higher than the concentration of contaminants. In our study, lower [persulfate]/[BA] ratios were employed such that BA would be the predominant $SO_4^{\bullet-}$ scavenger. This approach allowed us to quantify and compare persulfate utilization efficiency and also to follow the formation of the breakdown products. The solution pH was buffered by 20 mM phosphate, and the pH was adjusted to an initial value of pH 7.5 using 1 M NaOH or 1 M H_2SO_4. The pH of solutions remained in the pH range 7.3 – 7.8 at all times during the course of the experiments. Experiments were carried out at ambient temperature (T = 22 ± 1°C) or in a water bath (T = 35, 50, and 70°C). At predetermined time intervals, 2 or 3 reactor tubes were sacrificed and the reactions were immediately quenched in an ice bath. Subsequently, aliquots were

subsampled from each test tube and analyzed for persulfate, benzoic acid and its oxidation products, and total organic carbon (TOC).

Regarding chlorendic acid (CA), the degradation of CA by heat-activated $S_2O_8^{2-}$ was observed in homogenous solutions (*i.e.*, solid-free solutions) to systematically investigate the effect of pH as well as solutes such as HCO_3^- and Cl^- on the rate of CA transformation. The experiments were conducted in 16 mL sealed test tubes that contained 10 mL of reaction solution. The solution was comprised of CA (50 - 100 µM), $S_2O_8^{2-}$ (1 mM), HCO_3^- (0 mM or 10 mM), chloride (0 mM or 5 mM), and benzoic acid (a model for competing contaminants, 10-100 µM). The solution pH was adjusted to pH 4 or 8 using 1 M H_2SO_4 or 1 M NaOH. The solution also contained 50 mM sodium sulfate, which served as background electrolyte to mitigate fluctuations in ionic strength caused by the production and consumption of ions.

Reactors were manually shaken daily and a water bath was used to control temperature to 40 or 70°C. In the case of room temperature experiments, reactors were placed on the bench. At predetermined time intervals, the activation of persulfate was quenched by submerging reactors in an ice bath, and the solution pH, oxidation-reduction potential (ORP), together with the concentrations of persulfate, chlorendic acid, chloride, chlorate, and total organic carbon (TOC) were measured. Experiments were performed in triplicate and average values along with one standard deviation are reported.

2.3 Analytical Methods

Persulfate was measured spectrophotometrically using a modification of the Kolthoff potassium iodide method (Kolthoff and Belcher, 1957). TOC was measured on a Shimadzu organic carbon analyzer. Aromatic compounds and other organic acids were analyzed on a Thermo Scientific Ultimate 3000 ultra-high performance liquid chromatograph (UHPLC) equipped with a UV/vis photodiode array detector. For benzoic acid, 1 mL samples were acidified with 50 μL of 1 M H_2SO_4 prior to analysis. In addition, 50 μL of methanol was added to each sample to quench any oxidation reactions between organic compounds of interest and persulfate. Organic compound separation was carried out using a 4.6 mm × 100 mm C18 5μm column. The mobile phase consisted of acetonitrile (ACN) and 1 mM H_2SO_4 and the chromatographic condition was programmed as follows: 1) minutes 0 – 3: 85% ACN, 15% of 1 mM H_2SO_4, flow rate of 0.7 mL/min; 2) between minutes 3 – 3.1, the flow rate was increased to 1 mL/min and was held at this value between minutes 3.1 and 6; 3) minutes 6 – 6.1: the eluent composition was changed to 70% ACN and 30% of 1mM H_2SO_4 and held at this composition until the end of the run. Benzoic acid and its transformation products were detected with UV absorbance detection at 235 nm (3-hydroxybenzoic acid), 255 nm (4-hydroxybenzoic acid), 271 nm (benzoic acid, phenol, catechol, and hydroquinone), and 303 nm (2-hydroxybenzoic acid).

In the case of the homogenous CA experiments, 1 mL samples were acidified with 50 μL of 1 M H_2SO_4 prior to HPLC analysis. In addition, 50 μL of methanol was added to each sample to quench any further oxidation reactions between CA and persulfate. The mobile

phase consisted of 70% ACN and 30% 1 mM H_2SO_4 at a flow rate of 0.8 mL/min. Chlorendic acid was detected with UV absorbance detection at 220 nm.

Experiments were conducted in duplicate or triplicate, and average values along with one standard deviation are reported.

3.0 Oxidation of Benzoic Acid by Heat-Activated Persulfate: Effect of Temperature on Transformation Pathway and Product Distribution

Reproduced with permission from Zrinyi, N; Pham, A.L.T. Oxidation of benzoic acid by heat-activated persulfate: effect of temperature on transformation pathway and product distribution. *Water Research* 2017, *120*, 43-51.

3.1 Introduction

Peroxydisulfate (or simply persulfate, $S_2O_8^{2-}$) is being increasingly used in advanced oxidation processes for treatment of wastewater and industrial waste, and *in situ* chemical oxidation (ISCO) for remediation of contaminated soil and groundwater (Huling et al., 2006; Tsitonaki et al., 2010; Deng and Ezyske, 2011; Siegrist et al., 2011; Drzewicz et al., 2012; Ahn et al., 2013; Yang et al., 2014; Lutze et al., 2015; Sun et al., 2016). In these applications, persulfate is activated into sulfate and hydroxyl radicals ($SO_4^{\bullet-}$ and $^{\bullet}OH$), powerful oxidants that can oxidize a wide range of organic contaminants. Common persulfate activators include heat (Waldemer et al., 2007; Johnson et al., 2009; Constanza et al., 2010), ultraviolet light (Yang et al., 2014; Sun et al., 2016), dissolved metals and metal oxides (Anipsitakis and Dionysiou, 2004; Ahmad et al., 2010; Sra et al., 2010; Drzewicz et al., 2012; Ahn et al., 2013; Liu et al., 2014), and alkaline solutions (Singh and Venkatarao, 1976; Furman et al., 2010).

Persulfate-based ISCO involves the injection of $S_2O_8^{2-}$ into the subsurface where it is activated by naturally present iron- and manganese-containing minerals, or by dissolved iron ions that are co-injected with $S_2O_8^{2-}$ (Tsitonaki et al., 2010). The injection of a base into the subsurface is also being employed to activate $S_2O_8^{2-}$, although the utility of this approach can be relatively limited at sites with strong natural buffering capacity (Tsitonaki

et al., 2010). Heat is another widely used $S_2O_8^{2-}$ activator in ISCO. *In situ* thermal activation of $S_2O_8^{2-}$ is achieved through various approaches including steam injection, hydrogen peroxide (H_2O_2) addition (the rapid decomposition of H_2O_2 releases heat) (Tsitonaki et al., 2010), or by the EK-TAP technology (Reynolds, 2014). EK-TAP employs direct current to electrokinetically (EK) enhance the migration of $S_2O_8^{2-}$ in the subsurface, and alternating current to heat the subsurface up and thermally activate persulfate (TAP) (Reynolds, 2014). A distinct feature of EK-TAP is that both the EK and the TAP processes use the same electrode wells: once the persulfate migration process is completed, the direct current is switched to alternating current to activate $S_2O_8^{2-}$.

Previous studies investigating the degradation of contaminants by heat-activated $S_2O_8^{2-}$ focused primarily on the effect of temperature on the rates of $S_2O_8^{2-}$ consumption and contaminant removal. In contrast, with only a few exceptions the influence of temperature on the nature and distribution of contaminant degradation products has received little attention. A recent study by Mora *et al.* (Mora et al., 2011) reported that the primary products generated when phenol was subjected to $S_2O_8^{2-}$ treatment at 70°C were polymer-type products, whereas room temperature treatments produced hydroxylated phenols (Anipsitakis et al., 2006; Mora et al., 2011). Temperature appeared to control the ratio between iodinated- and brominated-disinfection products (I-DBPs and Br-DBPs) when a surface water sample was treated with $S_2O_8^{2-}$ (Chu et al., 2016). In this study, I-DBPs were the predominant products at T < 35°C whereas the Br-DBPs became increasingly important at above 35°C. Collectively, these observations are significant for the design and operation of persulfate-based treatment systems, and suggest that the

role of temperature in the $S_2O_8^{2-}$-based treatment systems beyond controlling the rate of persulfate activation merits further investigation.

In this study, through the transformation of benzoic acid we reported and discussed how temperature can affect the pathways through which contaminants are transformed and the distribution of breakdown products in heat-activated persulfate systems. Benzoic acid (BA) was chosen as a model compound for the following reasons: 1) the oxidation reactions of BA by $^{\bullet}OH$ and $SO_4^{\bullet-}$ are relatively well-characterized: whereas $^{\bullet}OH$ oxidizes BA via a hydroxylation mechanism (*e.g.*, Zhou and Mopper, 1990), $SO_4^{\bullet-}$ oxidizes BA via a hydroxylation and Kolbe-type decarboxylation mechanisms (Madhavan et al., 1978; Zemei and Fessenden, 1978). The studies by Madhavan et al. and Zemei and Fessenden suggested that the decarboxylation of BA by $SO_4^{\bullet-}$ produces a phenyl radical ($C_6H_5^{\bullet}$). We note that the subsequent fate of $C_6H_5^{\bullet}$ and factors affecting the branching between the hydroxylation and decarboxylation reactions were not discussed in those studies; 2) BA has been used as a model for the aromatic fraction of naphthenic acids (Yang et al. 2014); and 3) BA and does not adsorb to glassware or volatilize at elevated temperature to an appreciable extent. This is particularly important because the loss of BA from the experimental solution can be attributable to transformation and not adsorption or volatilization.

We measured the rates of persulfate consumption, BA degradation, and product formation to establish the reaction kinetics and transformation mechanism. The transformation branching under different temperatures was investigated via establishing

the time-concentration profiles of the products. In addition, the persulfate utilization efficiency, defined as the amount of benzoic decomposed per mole of persulfate consumed, was used to compare the efficiency of the persulfate treatment at different temperatures.

3.2 Materials and Methods

3.2.1 Chemicals

All chemicals were of ACS reagent grade and were used without further purification. Benzoic acid, potassium persulfate, potassium iodide, potassium phosphate, and sodium bicarbonate were obtained from VWR International. Other organic compounds (o, m, p-hydroxybenzoic acids, phenol, catechol, hydroquinone, 4-nitrobenzoic acid) were obtained from Sigma-Aldrich. All solutions were prepared using 18.2 MΩ·cm water (Millipore System).

3.2.2 Experimental Setup

Persulfate activation and benzoic acid (BA) oxidation experiments were conducted in 16 mL sealed test tubes that contained 10 mL of reaction solution. The initial concentrations of BA and persulfate were 0.1 – 5 mM and 1 mM, respectively. In remediation practice, the concentration of persulfate is usually much higher than the concentration of contaminants. In our study, lower [persulfate]/[BA] ratios were employed such that BA would be the predominant $SO_4^{\bullet-}$ scavenger. This approach allowed us to quantify and compare persulfate utilization efficiency and also to follow the formation of the breakdown products. The solution pH was buffered by 20 mM phosphate, and the pH was adjusted to an initial value of pH 7.5 using 1 M NaOH or 1 M H_2SO_4. The pH of solutions

remained in the pH range 7.3 – 7.8 at all times during the course of the experiments. Experiments were carried out at ambient temperature (T = 22 ± 1°C) or in a water bath (T = 35, 50, and 70°C). At predetermined time intervals, 2 or 3 reactor tubes were sacrificed and the reactions were immediately quenched in an ice bath. Subsequently, aliquots were subsampled from each test tube and analyzed for persulfate, benzoic acid and its oxidation products, and total organic carbon (TOC).

3.2.3 Analytical Methods

Persulfate was measured spectrophotometrically using a modification of the Kolthoff potassium iodide method (Kolthoff and Belcher, 1957). TOC was measured on a Shimadzu organic carbon analyzer. Aromatic compounds were analyzed on a Thermo Scientific Ultimate 3000 ultra-high performance liquid chromatograph (UHPLC) equipped with a UV/vis photodiode array detector. Prior to analysis, 1 mL samples were acidified with 50 μL of 1 M H_2SO_4. In addition, 50 μL of methanol was added to each sample to quench any oxidation reactions between organic compounds of interest and persulfate. Organic compound separation was carried out using a 4.6 mm × 100 mm C18 5μm column. The mobile phase consisted of acetonitrile (ACN) and 1 mM H_2SO_4 and the chromatographic condition was programmed as follows: 1) minutes 0 – 3: 85% ACN, 15% of 1 mM H_2SO_4, flow rate of 0.7 mL/min; 2) between minutes 3 – 3.1, the flow rate was increased to 1 mL/min and was held at this value between minutes 3.1 and 6; 3) minutes 6 – 6.1: the eluent composition was changed to 70% ACN and 30% of 1mM H_2SO_4 and held at this composition until the end of the run. Benzoic acid and its transformation products were detected with UV absorbance detection at 235 nm (3-hydroxybenzoic acid), 255 nm (4-

hydroxybenzoic acid), 271 nm (benzoic acid, phenol, catechol, and hydroquinone), and 303 nm (2-hydroxybenzoic acid).

Experiments were conducted in duplicate or triplicate, and average values along with one standard deviation are reported.

3.3 Results and Discussion

3.3.1 Effect of Temperature and Benzoic Acid Concentration on Rate of Persulfate Loss

Persulfate decomposition took place over a period of several hours to months (Figure 3.1A). Consistent with the results reported in previous studies (*e.g.*, House, 1962; Johnson et al., 2009), the $S_2O_8^{2-}$ decomposition rate increased with temperature. In the presence of an initial BA concentration 2 mM, the half-lives of $S_2O_8^{2-}$ decomposition were approximately 3465, 433, 51, and 3.3 h in the T = 22, 35, 50, and 70°C experiments, respectively. In addition, an increase in $[BA]_0$ resulted in a faster $S_2O_8^{2-}$ loss (Figure 3.1B). Previous studies also observed that an increase in the concentration of organic compounds accelerated the rate of $S_2O_8^{2-}$ loss, presumably due to radical chain reactions that propagated $S_2O_8^{2-}$ decomposition (*e.g.*, Liang et al., 2009; Liu et al., 2014). The mechanism through which BA accelerated the decomposition of $S_2O_8^{2-}$ is discussed in section 3.3.3.

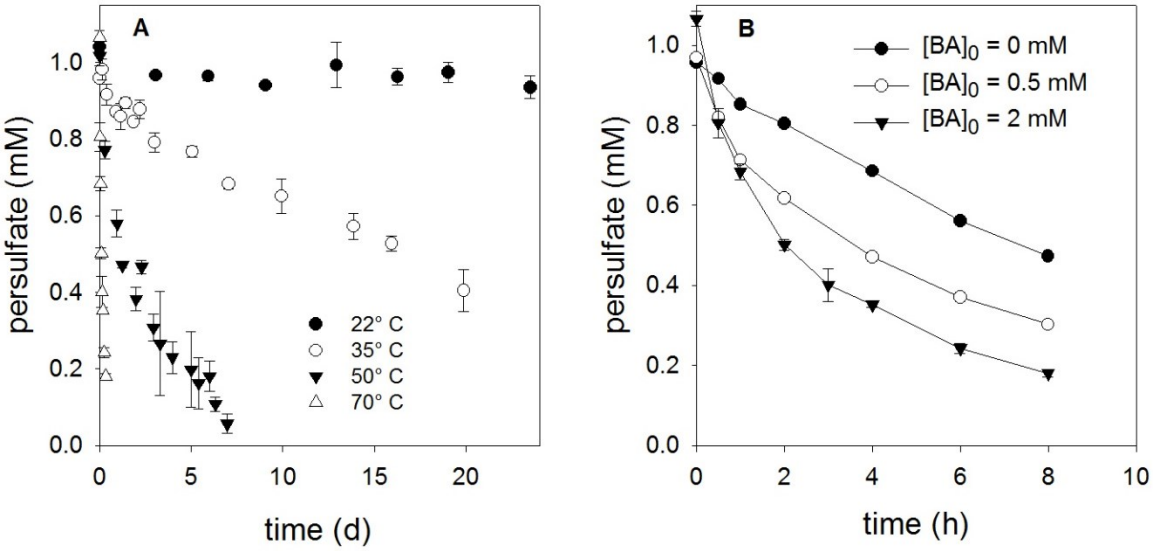

Figure 3.1: **A**: Persulfate decomposition at different temperatures; $[S_2O_8^{2-}]_0$ = 1 mM, $[BA]_0$ = 2 mM. **B**: Persulfate decomposition at different initial concentrations of benzoic acid (BA); T = 70°C, $[S_2O_8^{2-}]_0$ = 1 mM. All experiments were buffered by 20 mM phosphate (pH = 7.3 – 7.8).

3.3.2 Benzoic Acid Degradation

BA loss was negligible at 70°C in the absence of $S_2O_8^{2-}$ (data not shown), suggesting that the loss in the presence of $S_2O_8^{2-}$ (Figure 3.2) was due to transformation and not adsorption or volatilization. The transformation of BA is attributable to the reaction between BA and $SO_4^{\bullet-}$ and $^{\bullet}OH$ radicals, which were produced from the heat-activated $S_2O_8^{2-}$:

$$S_2O_8^{2-} \rightarrow 2SO_4^{\bullet-} \qquad k_1^{*} \qquad (3.1)$$

$$SO_4^{\bullet-} + H_2O \rightarrow {}^{\bullet}OH + SO_4^{2-} + H^+ \qquad k_2 < 6\times10^1\ M^{-1}s^{-1} \qquad (3.2)$$

$$SO_4^{\bullet-} + OH^- \rightarrow {}^{\bullet}OH + SO_4^{2-} \qquad k_3 = 6\times10^7\ M^{-1}s^{-1} \qquad (3.3)$$

$$SO_4^{\bullet-} + benzoic\ acid \rightarrow products \qquad k_4 = 1.2\times10^9\ M^{-1}s^{-1} \qquad (3.4)$$

$${}^{\bullet}OH + benzoic\ acid \rightarrow products \qquad k_5 = 5.9\times10^9\ M^{-1}s^{-1} \qquad (3.5)$$

*The value of k_1 depends on the solution temperature and composition. The values for k_2-k_5 were obtained from Neta et al. (Neta et al., 1988). These values were measured at T = 25°C.

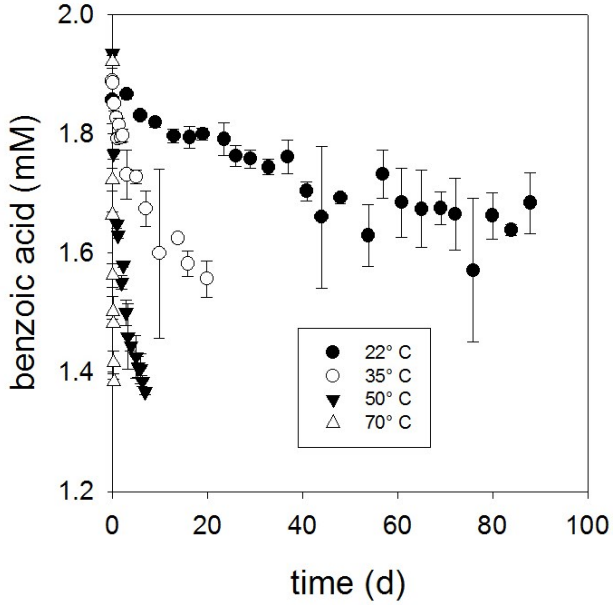

Figure 3.2: Benzoic acid degradation at different temperatures. $[S_2O_8^{2-}]_0$ = 1 mM, $[BA]_0$ = 2 mM, pH = 7.3 – 7.8 (buffered by 20 mM phosphate).

In the case of the room temperature experiment, the contribution of $^{\bullet}OH$ and $SO_4^{\bullet-}$ to the oxidation of BA can be estimated by comparing the steady state concentration of each radical. When $[BA]_0$ = 2 mM, BA should be the primary $SO_4^{\bullet-}$ and $^{\bullet}OH$ scavenger, because these radicals react much slower with other solutes present in the solution (*i.e.*, phosphate buffer, $S_2O_8^{2-}$, H_2O and OH^-). Therefore, the concentration of $^{\bullet}OH$ can be calculated according to the following equation:

$$\frac{d[HO^{\bullet}]}{dt} = rate\ of\ formation - rate\ of\ loss$$

$$\frac{d[HO^{\bullet}]}{dt} = k_2[H_2O][SO_4^{\bullet-}] + k_3[OH^-][SO_4^{\bullet-}] - k_5[BA][^{\bullet}OH]$$

At steady state:

$$[^{\bullet}OH] = [SO_4^{\bullet-}]\frac{k_2[H_2O]+k_3[OH^-]}{k_5[BA]}$$

When pH = 7.5 and $[BA]_0$ = 2 mM, using the k values above it is predicted that $[SO_4^{\bullet-}]_{ss}$ should be 3000 times greater than $[^{\bullet}OH]_{ss}$. Therefore, the rate of BA oxidation by $SO_4^{\bullet-}$ should be approximately 600 times faster than that by $^{\bullet}OH$. In the case of the 35 – 70°C experiments, it was not possible to compare $[^{\bullet}OH]_{ss}$ and $[SO_4^{\bullet-}]_{ss}$ using the approach above because the k values at these temperature are not available. To investigate the importance of $^{\bullet}OH$ and $SO_4^{\bullet-}$ at 70°C, the degradation of BA was investigated in the presence of 4-nitrobrenzoic acid (NBA), which is a compound that reacts quickly with $^{\bullet}OH$ (k_{OH} = 2.6×10^9 $M^{-1}s^{-1}$) but very slowly with $SO_4^{\bullet-}$ ($k_{SO4} \leq 10^6$ $M^{-1}s^{-1}$) (Neta et al., 1988). As can be seen from Figure 3.3, the presence of NBA slightly retarded the rate of BA degradation, suggesting that $^{\bullet}OH$ might have contributed to the oxidation of BA. However, $[^{\bullet}OH]_{ss}$ in this experiment must have been very small because only less than 1% of the initial NBA was degraded. Therefore, the transformation of BA in the 70°C experiment is mainly attributable to the reaction with $SO_4^{\bullet-}$.

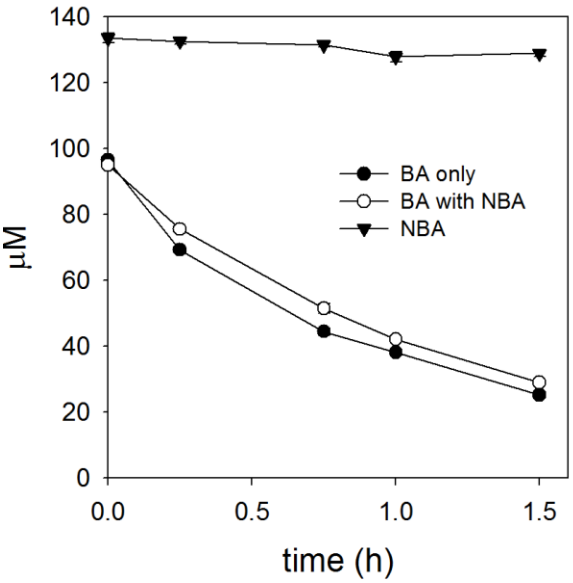

Figure 3.3: Benzoic acid (BA) degradation in the absence and presence of 4-nitrobenzoic acid (NBA). $[S_2O_8^{2-}]_0$ = 1 mM, pH = 7.3 – 7.8, $[BA]_0$ = 0.1 mM, $[NBA]_0$ = 0.13 mM.

3.3.3 Product Formation and Transformation Mechanism

Concurrent with the disappearance of benzoic acid was the formation of a suite of products. The products that were identified by HPLC/UV-vis are phenol, catechol, hydroquinone, and hydroxybenzoic acids (o-, m-, and p-HBA) (Figure 3.4). The mechanism through which these products are formed is proposed as follows. Unlike the reaction between BA and $^{\bullet}OH$ which results in the addition of a hydroxyl group to the aromatic ring (Zhou and Mopper, 1990), the reaction between BA and $SO_4^{\bullet-}$ proceeds via a one electron transfer step that produces a carboxyphenyl radical intermediate (reaction *6* in Scheme 3.1). According to the previous studies (Madhavan et al., 1978; Zemei and Fessenden, 1978), the carboxyphenyl radical then either undergoes decarboxylation to produce a phenyl radical $C_6H_5^{\bullet}$ (reaction *7*), or reacts with H_2O to produce a hydroxycyclohexadienyl radical (reaction *8*). Upon reacting with an oxidant (*e.g.*, O_2 and/or $S_2O_8^{2-}$), the hydroxycyclohexadienyl radical is converted into o-, m-, and p-HBAs (reactions *19* and *20*).

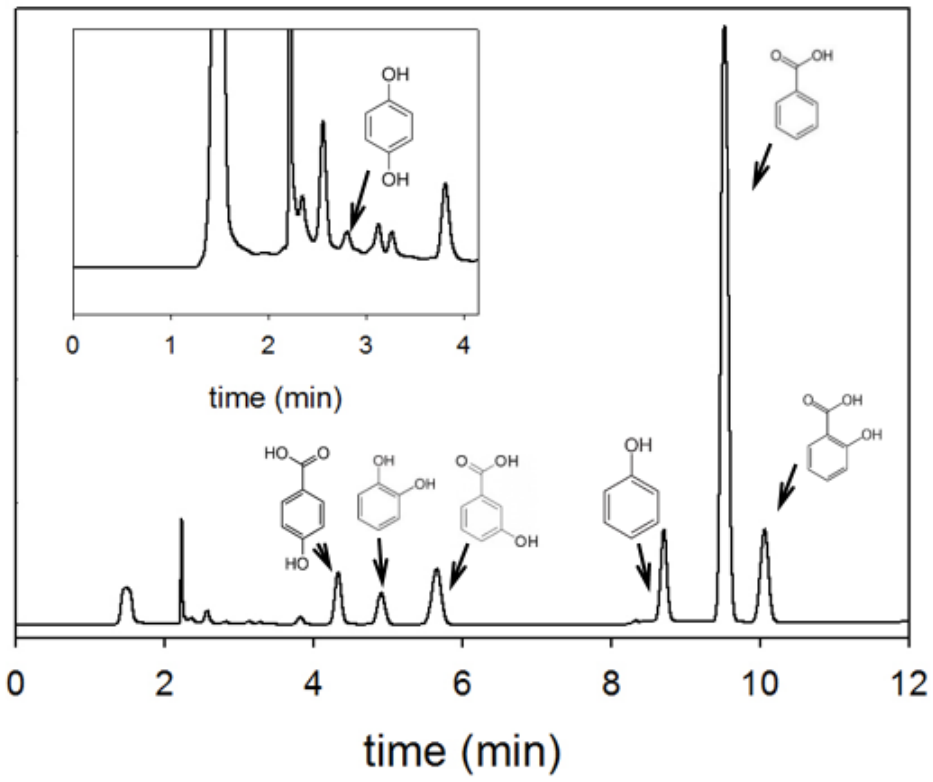

Figure 3.4: A typical HPLC chromatogram of samples taken from the benzoic acid oxidation experiments. The identified byproducts were phenol, catechol, hydroquinone, o-hydroxybenzoic acid, m-hydroxybenzoic acid, and p-hydroxybenzoic acid.

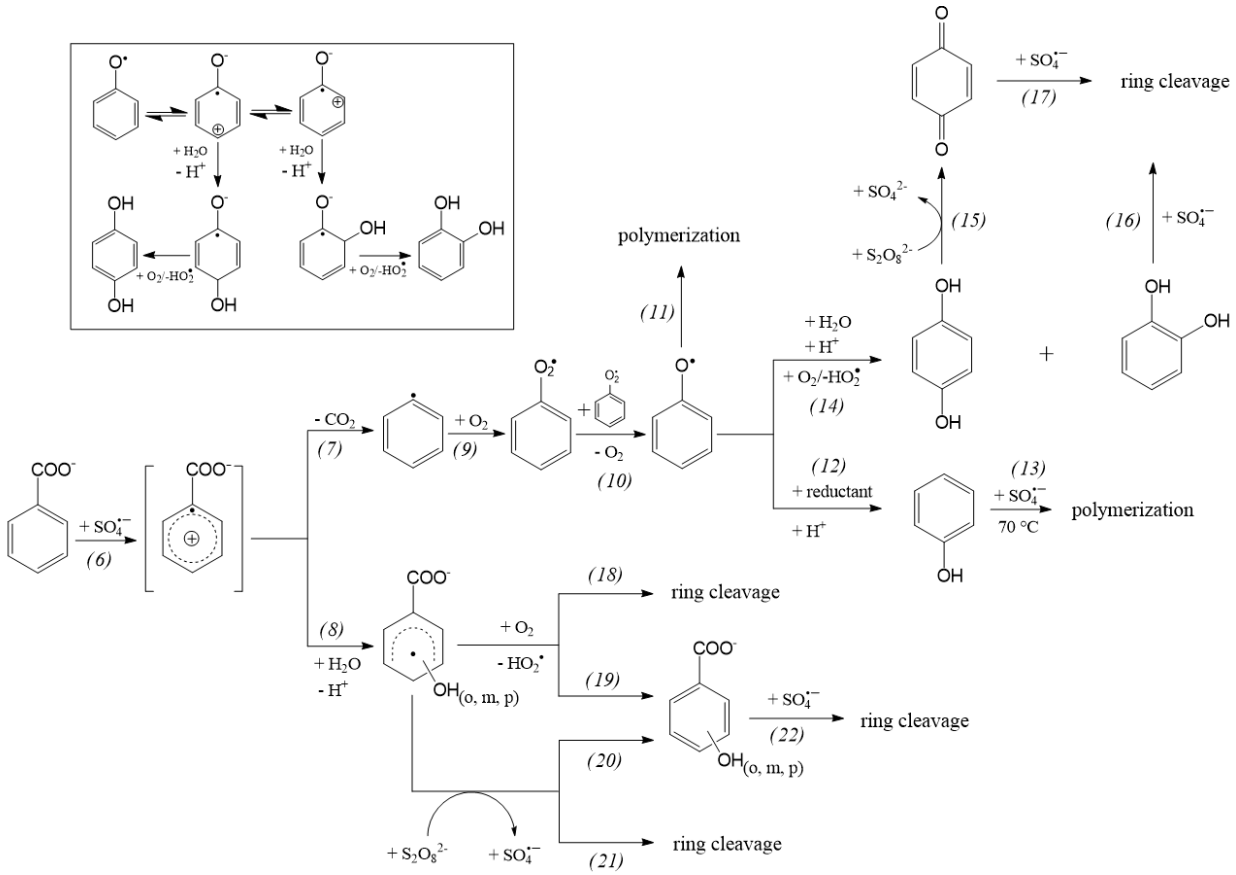

Scheme 3.1: Mechanism of benzoic acid transformation by heat-activated persulfate. Inset: the mechanism through which hydroquinone and catechol are formed from the phenoxyl radical.

The fate of the phenyl radical, $C_6H_5^{\bullet}$, was not discussed in the previous studies. The formation of phenol, catechol, and hydroquinone, namely the aromatic compounds that did not retain the carboxylic group, suggests that these products must have been produced from $C_6H_5^{\bullet}$. This transformation is proposed as follows. In the first step, $C_6H_5^{\bullet}$ reacts with O_2 to generate a peroxyl radical $C_6H_5O_2^{\bullet}$ (reaction *9*). This is likely a fast reaction as the reaction rate constants between carbon-centered radicals ($R^{\bullet}$) and O_2 are typically in the order of 10^9 $M^{-1}s^{-1}$ (Adams and Willson, 1969). Subsequently, $C_6H_5O_2^{\bullet}$ undergoes bimolecular disproportionation to form a phenoxyl radical $C_6H_5O^{\bullet}$ (reaction *10*). Further, $C_6H_5O^{\bullet}$ can either undergo radical coupling to give dimer-type products

(reaction *11*), or can react with other constituents in the solution. The reaction between phenoxyl radicals and reductants can generate phenolate ions (Neta et al., 1988). In our system, it is not clear which solute reacted with $C_6H_5O^{\bullet}$ to produce phenol (reaction *12*).

In $^{\bullet}OH$-based oxidative systems, catechol and hydroquinone are often direct products of phenol oxidation (*e.g.*, Zazo et al., 2005). This is not the pathway through which catechol and hydroquinone were formed in our system because the oxidation of phenol by $S_2O_8^{2-}$ at T = 70°C did not produce these compounds (Figure 3.5). This result is consistent with that of Mora *et al.* who proposed that the oxidation of phenol by $S_2O_8^{2-}$ at 70°C primarily produced polymer-type products (reaction *13* in Scheme 3.1) (Mora et al., 2011). The oxidation of HBAs (*i.e.*, the other direct products of BA oxidation) did not generate catechol and hydroquinone either (Figure 3.5). Therefore, the catechol and hydroquinone in our system most likely came directly from $C_6H_5O^{\bullet}$. This transformation, represented by reaction *14* and described in more detail in the inset of Scheme 3.1 consists of multiple rearrangement, addition and elimination steps (Altwicker, 1967).

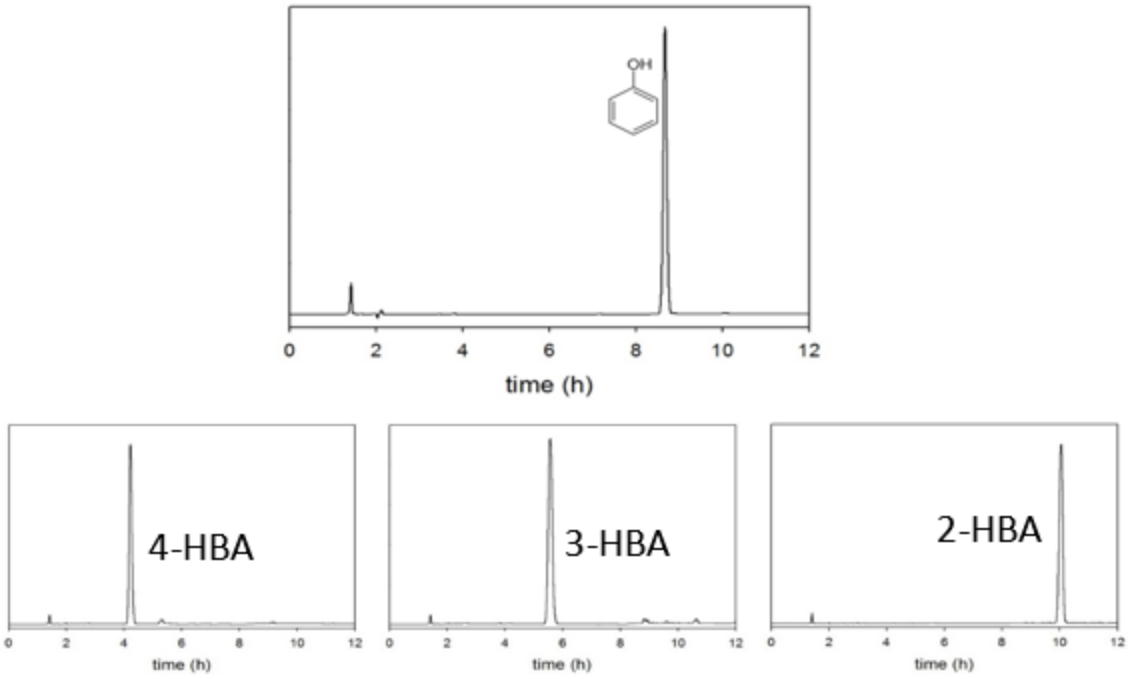

Figure 3.5: A typical HPLC chromatogram of samples taken from the phenol hydroxybenzoic acid oxidation experiments. The chromatogram suggests that catechol, hydroquinone, as well as other hydroxylated aromatic compounds, were not produced when phenol or HBAs were oxidized by $SO_4^{\bullet-}$. $[S_2O_8^{2-}]_0$ = 1 mM, $[2\text{-HBA}]_0$, $[3\text{-HBA}]_0$, or $[4\text{-HBA}]_0$ = 2 mM, pH = 7.3 – 7.8 (buffered by 20 mM phosphate), T = 70 ºC.

The involvement of the $C_6H_5O^{\bullet}$ radical in the transformation scheme is further supported by an experiment in which the transformation of BA was investigated in the presence of 2 μM $CuCl_2$. In this experiment, phenol exhibited a time-concentration profile similar to that in the absence of Cu(II), but neither catechol nor hydroquinone were formed (Figure 3.6). The cupric ion, a superoxide dismutase (Zafirou et al., 1998), must have reacted with the $C_6H_5O_2^{\bullet}$ radical and converted it into a $C_6H_5^{+}$ carbocation (Reaction 3.6). Upon reacting with H_2O, the $C_6H_5^{+}$ is converted into phenol (Reaction 3.7), but not catechol or hydroquinone.

$$C_6H_5O_2^{\bullet} + \mathrm{Cu(II)} \rightarrow C_6H_5^{+} + O_2 + Cu(I) \quad (3.6)$$

$$C_6H_5^{+} + H_2O \rightarrow C_6H_5\mathrm{OH} + H^{+} \quad (3.7)$$

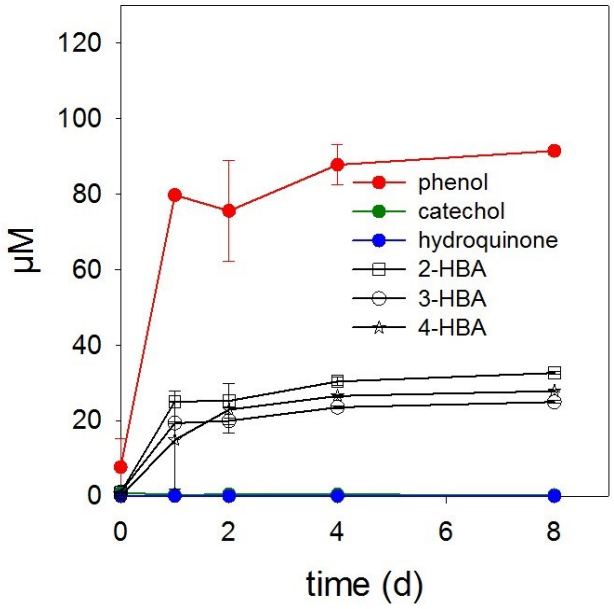

Figure 3.6: Evolution of aromatic byproducts produced from the oxidation of benzoic by persulfate in the presence of 2 µM $CuCl_2$. T = 70°C, $[S_2O_8^{2-}]_0$ = 1 mM, $[BA]_0$ = 2 mM, pH = 7.3 – 7.8 (buffered by 20 mM phosphate).

The time-concentration profiles of the decarboxylated products are distinct from each other (Figure 3.7). Whereas the concentration of phenol progressively increased, the concentration of catechol first increased then plateaued (in the T = 70°C experiment) or decreased (in the T = 22, 35, 50°C experiments). In all experiments, hydroquinone was always detected but its concentration never exceeded 3 µM. These results suggest that catechol and hydroquinone underwent further transformation (reactions *15* and *16* in Scheme 3.1). The experiments testing the reactivity of catechol and hydroquinone with $S_2O_8^{2-}$ suggest that hydroquinone is very reactive with $S_2O_8^{2-}$. At room temperature, hydroquinone was converted into benzoquinone within minutes (Figure 3.8). This observation is consistent with the fact that hydroquinone never accumulated in the BA experiments. Therefore, the transformation of hydroquinone is attributable to the oxidation by $S_2O_8^{2-}$ via a two-electron transfer reaction (reaction *15*) rather than by

$SO_4^{\bullet-}$. In contrast, phenol and catechol did not appreciably react with $S_2O_8^{2-}$ at room temperature, and were oxidized (most likely by $SO_4^{\bullet-}$) at similar rates at T = 70°C (Figure 3.9). Therefore, the transformation of phenol and catechol is attributable to their reaction with $SO_4^{\bullet-}$ (reactions *13* and *16,* respectively).

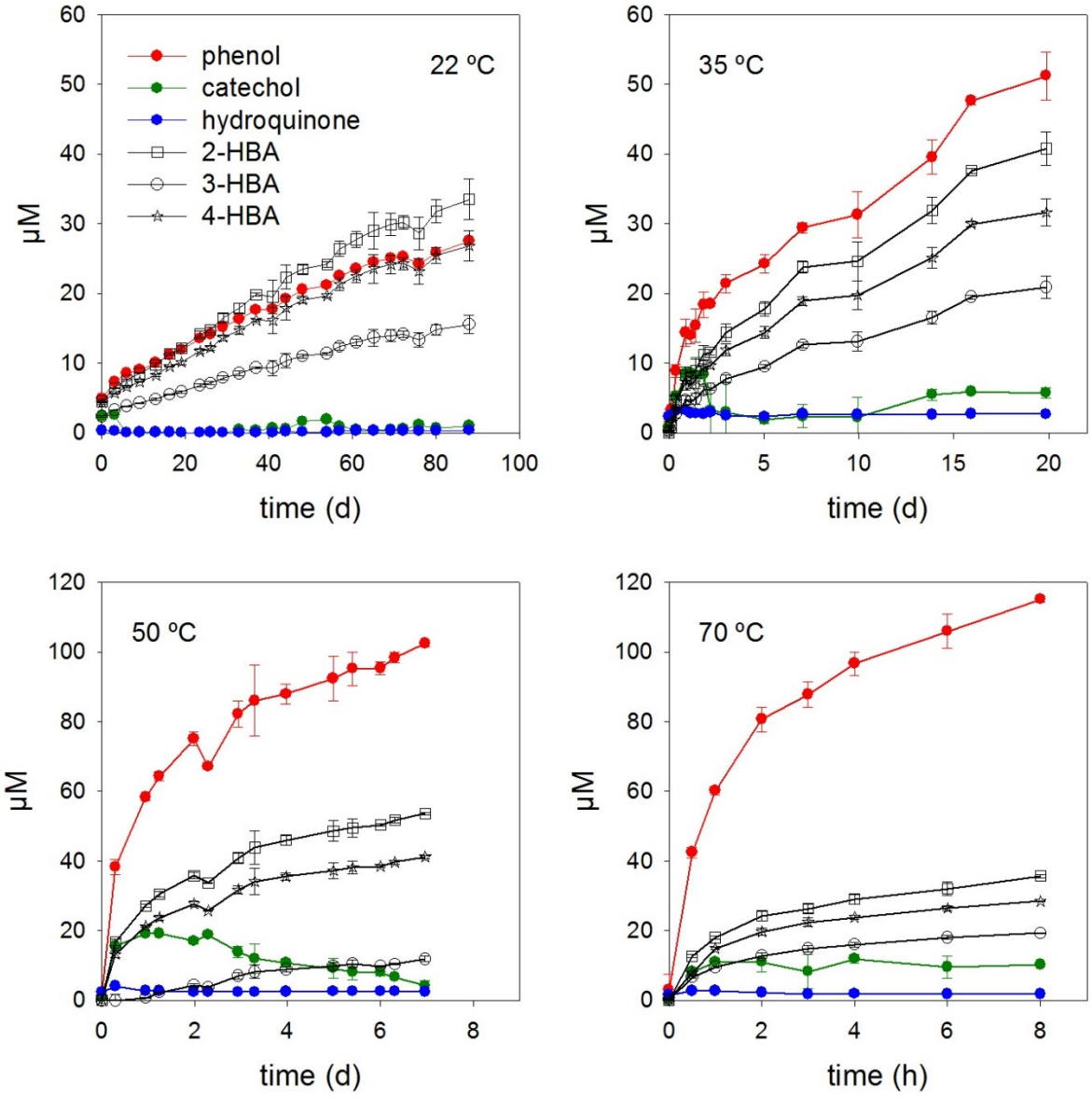

Figure 3.7: Evolution of aromatic byproducts produced from the oxidation of benzoic by heat-activated persulfate at T = 22 – 70°C. $[S_2O_8^{2-}]_0$ = 1 mM, $[BA]_0$ = 2 mM, pH = 7.3 – 7.8 (buffered by 20 mM phosphate). Note that these figures have different axis scales.

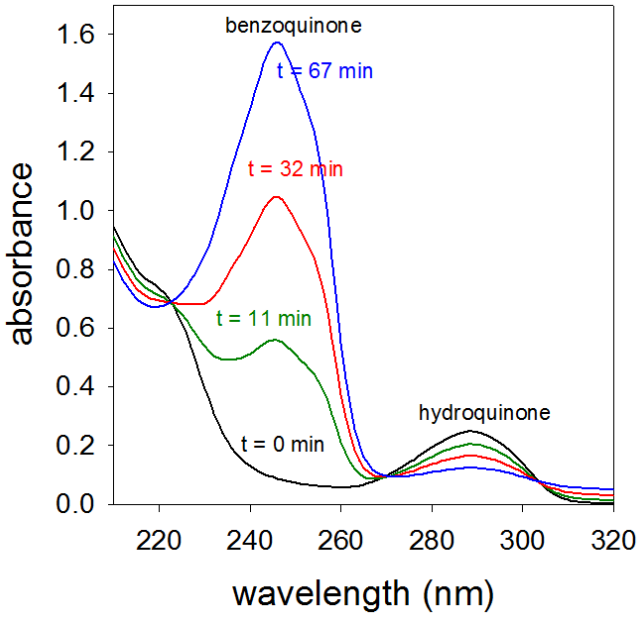

Figure 3.8: Uv-vis spectra of samples taken from the 1,4-hydroquinone oxidation experiment. $[S_2O_8^{2-}]_0$ = 1 mM, $[hydroquinone]_0$ = 0.1 mM, pH = 7.3 – 7.8, T = 22°C.

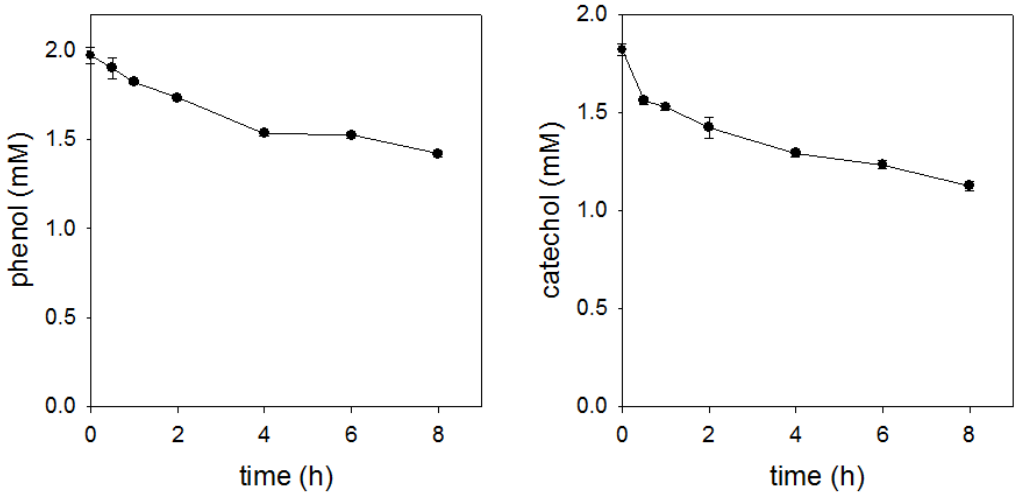

Figure 3.9: Phenol (left) and catechol (right) loss. $[S_2O_8^{2-}]_0$ = 1 mM, pH = 7.3 – 7.8 (buffered by 20 mM phosphate), T = 70 ºC.

The identified products only accounted for 35 – 50% of the amount BA degraded (Figure 3.10). The unaccounted products could be polymer-type (produced from reactions *11* and *13*) and/or ring-cleavage ones. The latter can be formed when one of the downstream products is further oxidized by $SO_4^{\bullet-}$ (*e.g.*, reactions *16*, *17*, *22*). The ring-cleavage

products also can be produced directly from the hydroxyhexadienyl radical when it reacts with O_2 or $S_2O_8^{2-}$ (reactions *18* and *21*) (Liu et al., 2016).

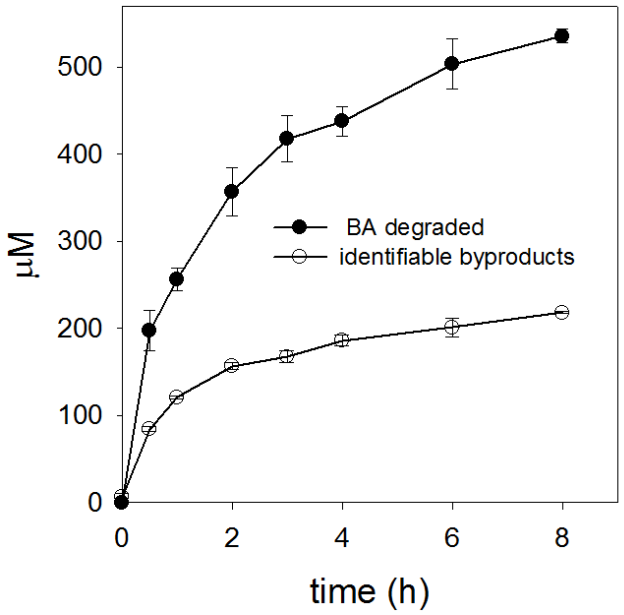

Figure 3.10: Evolution of total concentration of aromatic byproducts compared to the total concentration of BA degraded. in the T = 70 ºC, $[S_2O_8^{2-}]_0$ = 1 mM, $[BA]_0$ = 2 mM, pH = 7.3 – 7.8 (buffered by 20 mM phosphate).

In the T = 70°C, $[BA]_0$ = 2 mM experiment, TOC decreased by approximately 10% (Figure 3.11). The decrease is only partially due to reaction 7 because the amount of TOC produced via decarboxylation does not account for the TOC loss measured experimentally. The initial TOC concentration in this experiment was $[TOC]_0$ = 12 (g C/mole) × 7 (# mole C/mole BA) × 2 mM BA = 168 mg C/L. At t = 8h, approximately 0.5 mM BA was degraded (Figure 3.1B in the main text). If the decarboxylation of BA were the only pathway that converted the organic carbon into CO_2, the TOC concentration at t = 8h would have been [TOC] = $[TOC]_0$ - 0.5 mM BA × 1 (# mole C eliminated via decarboxylation/mole BA) × 12 (g C/mole) = 168 - 6 = 162 mg C/L, *i.e.*, $[TOC]_{t = 8h}$ = 97% $[TOC]_0$. The measured $[TOC]_{t = 8h}$ was approximately $[TOC]_{t = 8h}$ = 90% $[TOC]_0$, suggesting

that decarboxylation of other compounds (*e.g.*, HBAs, ring-cleavage products) also must have happened.

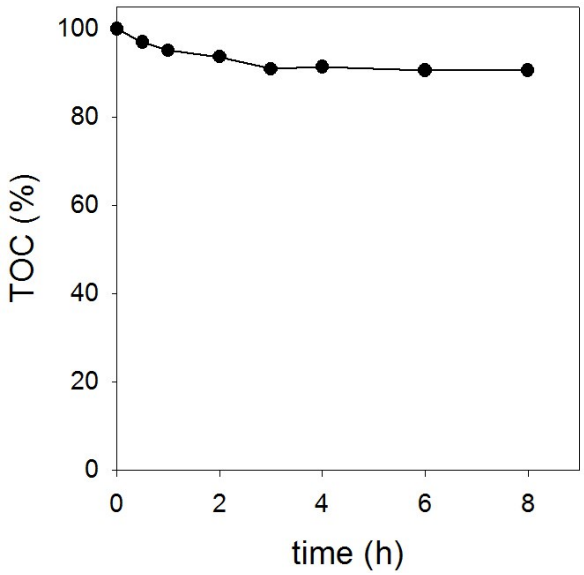

Figure 3.11: Total organic carbon (TOC) loss in the benzoic acid oxidation experiment. $[S_2O_8^{2-}]_0$ = 1 mM, $[BA]_0$ = 2 mM, pH = 7.3 – 7.8 (buffered by 20 mM phosphate).

In the proposed mechanism, reactions *15*, *20,* and *21* and are responsible for the $S_2O_8^{2-}$ loss along with the loss due to reaction *1*. An increase in the BA concentration would have increased the formation rates of hydroxyhexadienyl radical, hydroquinone, and benzoquinone, thereby accelerating the decomposition of $S_2O_8^{2-}$ (Figure 3.1B). It is noted that reactions *15*, *20*, and *21* may not be the only ones that accelerated the decomposition of $S_2O_8^{2-}$. In this very complex system of many radical and organic species, the faster $S_2O_8^{2-}$ decomposition at higher BA concentrations could also have arisen from other radical and non-radical reactions that can propagate the decomposition of $S_2O_8^{2-}$. For example, the accelerated activation of persulfate could also have been due to the reaction with semiquinone radical, which is produced from the comproportionation

reaction between hydroquinone and benzoquinone (Fang et al., 2013). The ability of other intermediates to activate $S_2O_8^{2-}$ also cannot be excluded (e.g. Ahmad et al., 2013 observed that phenolates were capable of activating $S_2O_8^{2-}$).

3.3.4 Effect of Temperature on the Distribution of Benzoic Acid Oxidation Products

Temperature influenced the distribution of the breakdown products (Figure 3.12). Specifically, phenol, the most prominent decarboxylated product, was produced significantly more at higher temperatures. Whereas at T = 70°C phenol was the most abundant product, 2-HBA was the most abundant product at T = 22°C. The concentration of phenol relative to those of other products progressively decreased with temperature (Figure 3.12). To gain further insights into the effect of temperature on the branching between the decarboxylation and hydroxylation of BA, we examined the time profile of the decarboxylation ratio (DR) and decarboxylation fraction (DF). DR is defined as the ratio between the total amount of the decarboxylated products (*i.e.*, phenol, catechol, and hydroquinone) and the total amount of the hydroxylated products (*i.e.*, HBAs), whereas DF is the ratio between the total amount of the decarboxylated products and the total amount of BA degraded. It is noted that these ratios are only approximate proxies for the branching between the decarboxylation and hydroxylation reactions because they do not account for the other products (*i.e.*, benzoquinone, polymer-type and ring-cleavage products). Also, as the transformation of BA took place at different rates, DR and DF were plotted against the reaction extent (*i.e.*, $[BA]/[BA]_0$) rather than time so that the comparisons were valid.

Both DR and DF increased as the temperature increased (Figure 3.12), suggesting that the decarboxylation was increasingly favourable at elevated temperatures. The branching between decarboxylation and hydroxylation could be attributable to the branching between reaction *7* and *8*. It is also possible that the change in the branching was due to a change in the contribution of $SO_4^{\bullet-}$ and $^{\bullet}OH$ to the overall transformation of BA (*i.e.*, more hydroxylation with increasing contribution of $^{\bullet}OH$ to the transformation of BA). However, the latter explanation is unlikely because, as mentioned earlier, the transformation of BA was mainly attributable to $SO_4^{\bullet-}$. Regardless of the mechanism, our results clearly demonstrate the effect of temperature on the distribution of the benzoic acid oxidation products.

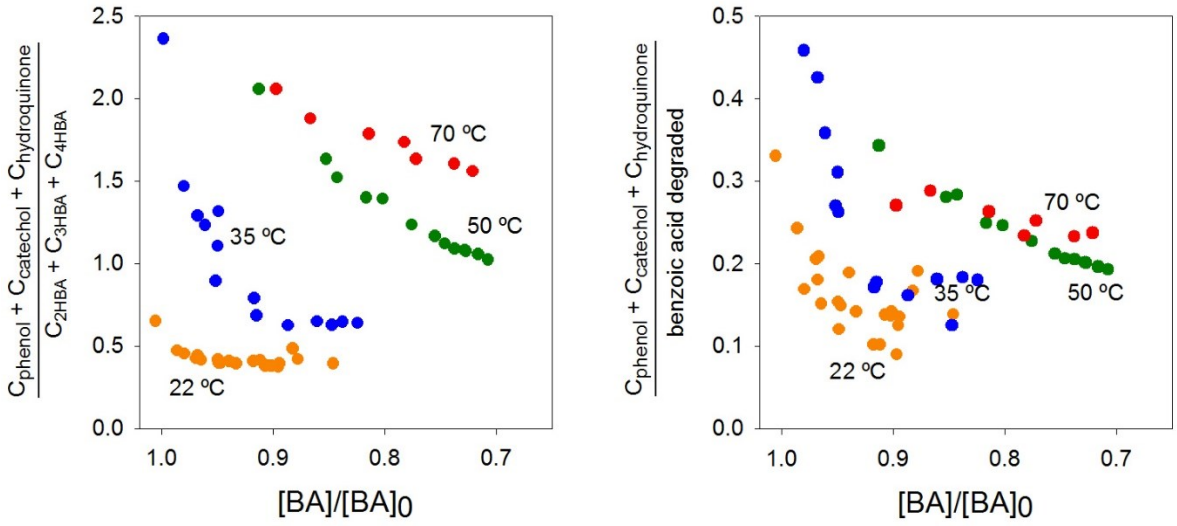

Figure 3.12: Effect of temperature on benzoic acid decarboxylation ratio (left) and fraction (right).

As the experiments progressed, DR and DF decreased notably. This trend is unlikely due to changes in the branching between decarboxylation and hydroxylation over time, but more likely due to the subsequent transformation of the decarboxylated products (*e.g.*,

reaction *15*) which lower their concentrations relative to those of the hydroxylated products.

3.3.5 Persulfate Utilization Efficiency

As described above, temperature, the concentration of BA, and the breakdown products affected the overall rate of persulfate consumption. To compare the persulfate utilization efficiency across different experimental conditions, the stoichiometric efficiency, E = (Δ[benzoic acid])/Δ[$S_2O_8^{2-}$]) × 100%, was calculated from the experimental data (Figure 3.13). Overall, the stoichiometric efficiency varied slightly with temperature although no clear temperature-efficiency trend was observed (see the E values of the $[BA]_0$ = 0.5 and 2 mM experiments in Figure 3.13). In general, an increase in the concentration of contaminants would lead to a higher persulfate utilization efficiency because more $SO_4^{\bullet-}$ will be scavenged by the contaminants than by the background solutes and the breakdown products. However, this was not always the case in our study. For example, in the T = 70°C experiments, E progressively increased as $[BA]_0$ increased from 0.5 to 5 mM. In contrast, in the T = 22°C experiments E slightly decreased when $[BA]_0$ increased from 0.5 mM to 2 mM. This difference could be attributable to the varying yield of $SO_4^{\bullet-}$ at different temperature. As noted in section 3.3.2, in our system persulfate was consumed via many reactions including reactions *1*, *15*, *20*, and *21*. These reactions yield different amounts of $SO_4^{\bullet-}$: in reaction *1* two moles of $SO_4^{\bullet-}$ are generated for every mole of $S_2O_8^{2-}$ consumed, in reactions *20* and *21* one mole of $SO_4^{\bullet-}$ is produced from one mole of $S_2O_8^{2-}$, whereas the consumption of $S_2O_8^{2-}$ via reaction *15* does not produce $SO_4^{\bullet-}$. When $[BA]_0$ and temperature varied, a change in the contribution of each of these reactions to the

overall consumption of $S_2O_8^{2-}$ would affect the $SO_4^{\bullet-}$ yield and, therefore, the stoichiometric efficiency E.

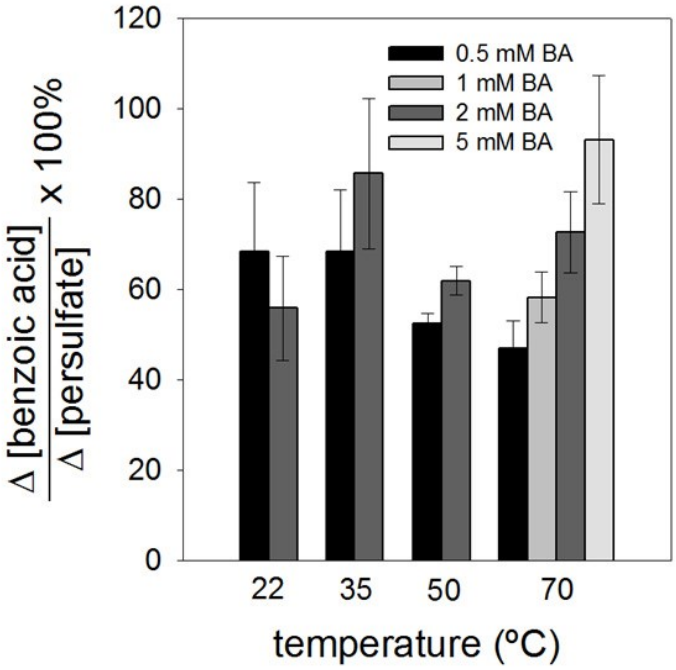

Figure 3.13: Effect of temperature and initial concentration of benzoic acid on stoichiometric efficiency. pH = 7.3 – 7.8, [phosphate] = 20 mM, T = 22 – 70°C, $[S_2O_8^{2-}]_0$ = 1 mM, $[BA]_0$ = 0.5 – 5 mM.

3.3.6 Implications for Heat-Activated Persulfate Treatment Systems

The results described above highlight the complexity of the heat-activated persulfate treatment system. Using the transformation of benzoic acid as a test case, we demonstrated the effect of temperature on not only the kinetics of $S_2O_8^{2-}$ activation but also on the contaminant transformation pathway and product distribution. When reacting with $SO_4^{\bullet-}$, BA underwent decarboxylation and hydroxylation to produce a suite of aromatic products. A fragmentation mechanism similar to the decarboxylation of BA was implicated in the debromination of bromobenzene, bromotoluene, and bromobenzoic acid (Madhavan et al., 1978). The transformation of polychlorinated biphenyls by $SO_4^{\bullet-}$ produced aromatic substances that contained fewer chlorine atoms

(Fang et al., 2013), presumably also via a fragmentation mechanism. For the derivatives of benzoic acid, it was shown that the branching between decarboxylation and other transformation pathways during oxidation with $SO_4^{\bullet-}$ depended on the nature and position of the ring substituents (Zemei and Fessenden, 1978). Our study showed that this branching also depended on the reaction temperature. Future research investigating the transformation of aromatics as well as other types of contaminants by heat-activated persulfate should consider the effect of temperature on the transformation pathway and product distribution.

The ability of $SO_4^{\bullet-}$ to initiate decarboxylation and the effect of temperature on this process can have important implications for various applications. For example, a recent study demonstrated that when pretreated with $SO_4^{\bullet-}$ natural organic matter (NOM) was more reactive with chlorine and exhibited higher disinfection product formation potential (Lu et al., 2016). It was postulated that the increased reactivity was the result of decarboxylation and subsequent formation of phenolic moieties within the NOM occurred through a mechanism that is similar to that proposed in our study. In that study, the activation of persulfate and pretreatment of NOM occurred at T = 70°C, and it is unclear to what extent the enhanced reactivity of NOM would have been observed at lower temperatures (*e.g.*, in systems in which persulfate is activated by UV light or by transition metals) (Lu et al., 2016). Another example is related to the treatment of perfluorinated carboxylic acids (PFCAs) by $SO_4^{\bullet-}$. The transformation PFCAs by UV/$S_2O_8^{2-}$ and heat/$S_2O_8^{2-}$ was proposed to occur via decarboxylation coupled with fragmentation, producing shorter chain compounds (Hori et al., 2007; Kutsuna and Hori, 2007; Hori et al.,

2008; Qian et al., 2016). We note that the influence of temperature on the transformation pathway and distribution of products were not discussed in these studies.

The relatively fast reaction between hydroquinone and un-activated $S_2O_8^{2-}$ observed in our study (reaction *15*) suggests that soil organic matter containing reduced quinone moieties will exert a significant oxidant demand, resulting in a rapid initial consumption of $S_2O_8^{2-}$ when it is injected into the subsurface. Remediation systems utilizing heat to activate $S_2O_8^{2-}$ may transform functional groups in soil organic matter into phenolate and quinone moieties, which can react with $S_2O_8^{2-}$ and further depress its concentration. These $S_2O_8^{2-}$ loss pathways, together with the losses due to reactions with reduced metals, should be considered when assessing $S_2O_8^{2-}$ longevity and contaminant transformation efficiency in persulfate-based ISCO.

3.4 Conclusions

This study investigated the oxidation of benzoic acid by heat-activated persulfate. Key findings and their implications are summarized below:

- The detailed pathway through which benzoic acid is oxidized by $SO_4^{\bullet-}$ was established, which showed that benzoic acid was concurrently transformed by a decarboxylation and a hydroxylation mechanisms. The ability of $SO_4^{\bullet-}$ to initiate decarboxylation reactions and, more broadly, fragmentation reactions, could be important to the transformation of a number of organic contaminants such as halogenated aromatic compounds and perfluorinated carboxylic acids.

- Temperature influenced the branching between the hydroxylation and decarboxylation mechanisms, and thus the distribution of benzoic acid transformation products. This finding, together with those reported by Mora *et al*. 2011 and Chu *et al.* 2016, suggests that in the persulfate-based treatment systems temperature controls not only the rates of persulfate activation but also the nature and distribution of breakdown products.

- The persulfate utilization efficiency, $E = (\Delta[\text{benzoic acid}])/\Delta[S_2O_8^{2-}]) \times 100\%$, did not vary appreciably with temperature. Depending on the persulfate activation temperature, an increase in the initial concentration of benzoic acid increased or decreased E. As was discussed in section 3.3.4, the yield of $SO_4^{\bullet-}$ was dependent on many factors, including the initial concentration of benzoic acid and its breakdown products. Future research will investigate if other types of contaminants exhibit a similar effect on the $SO_4^{\bullet-}$ yield and the persulfate utilization efficiency.

3.5 References

Adams, G. E., Willson, R. L., 1969. Pulse radiolysis studies on the oxidation of organic radicals in aqueous solution. *Transaction of the Faraday Society*, 65, 2981-2987.

Ahmad, M., Teel, A. L., Watts, R. J., 2010. Persulfate activation by subsurface minerals. Journal of *Contaminant Hydrology*, 115, 34-45.

Ahmad, M., Teel, A. L., Watts, R. J., 2013. Mechanism of persulfate activation by phenols. *Environmental Science & Technology*, 47, 5864-5871.

Ahn, S., Peterson, T. D., Righter, J., Miles, D. M., Tratnyek, P. G., 2013. Disinfection of ballast water with iron activated persulfate. *Environmental Science & Technology*, 47, 11717-11725.

Altwicker, E. R. The chemistry of stable phenoxy radicals. Chemical Reviews. 1967, 67, 475-531.

Anipsitakis, G. P., Dionysiou, D. D., 2004. Radical generation by the interaction of transition metals with common oxidants. *Environmental Science & Technology*, 38, 3705-3712.

Anipsitakis, G. P., Dionysiou, D. D., Gonzalez, M. A., 2006. Cobalt-mediated activation of peroxymonosulfate and sulfate radical attack on phenolic compounds: Implications of chloride ions. *Environmental Science & Technology*, 40, 1000-1007.

Chu, W., Hu, J., Bond T., Gao, N., Xu, B., Yin D., 2016. Water temperature significantly impacts the formation of iodinated haloacetamides during persulfate oxidation. *Water Research*, 47-55.

Constanza, J., Otano, J. C., Pennell, K. D., 2010. PCE oxidation by sodium persulfate in the presence of soils. *Environmental Science & Technology*, 44, 9445-9450.

Deng, Y., Ezyske, C. M., 2011. Sulfate radical-advanced oxidation process (SR-AOP) for simultaneous removal of refractory organic contaminants and ammonia in landfill leachate. *Water Research*, 45 (18), 6189-6194.

Drzewicz, P., Perez-Estrada, L. A., Alpatova, A., Martin, J. W., El-Din, M. G, 2012. Impact of peroxydisulfate in the presence of zero valent iron on the oxidation of cyclohexanoic acid and naphthenic acids from oil sands process-affected water. *Environmental Science & Technology*, 46, 8984-8991.

Fang, G. D., Dionysiou, D. D., Zhou, D. M., Wang, Y., Zhu, X. D., Fan, J. X., Cang, L., Wang, Y. J., 2013. Transformation of polychlorinated biphenyls by persulfate at ambient temperature. *Chemosphere*, 90, 1573-1580.

Furman, O. S., Teel, A. L., Watts, R. J., 2010. Mechanism of base activation of persulfate. *Environmental Science & Technology*, 44, 6423-6428.

Hori, H., Ari, Y., Hayakawa, E., Taniyasu, S., Yamashita, N., Kutsuna, S., 2007. Efficient decomposition of environmentally persistent perfluorocarboxylic acids by use of persulfate as a photochemical oxidant. *Environmental Science & Technology*, 39, 2383-2388.

Hori, H., Ari, Y., Nagaoka, Y., Murayama, M., Kutsuna, S., 2008. Efficient decomposition of perfluorocarboxylic acids and alternative fluorochemical surfactants in hot water. *Environmental Science & Technology*, 42, 7438-7443.

House, D. A., 1962. Kinetics and mechanism of oxidations by peroxydisulfate. *Chemical Reviews*, 62, 185-203.

Huling, S. G., Pivetz, B. E., 2006. In-Situ Chemical Oxidation. U.S. Environmental Protection Agency Engineering Issue. https://archive.epa.gov/ada/web/html/isco.html.

Johnson, R. L., Tratnyek, P. G., Johnson, R. O., 2009. Persulfate persistence under thermal activation conditions. *Environmental Science & Technology*, 42, 9350-9356.

Kolthoff, I. M., Belcher, R., 1957. Volumetric Analysis, Volume III, Titration Methods: Oxidation-Reduction Reactions, John Wiley & Sons, Inc, New York, pp. 287-291.

Kutsuna, S., Hori, H., 2007. Rate constants for aqueous-phase reactions of $SO_4^{\bullet-}$ with $C_2F_5C(O)O^-$ and $C_3F_7C(O)O^-$ at 298 K. *International Journal of Chemical Kinetics*, 39, 276–288.

Liang, C., Su, H., 2009. Identification of Sulfate and Hydroxyl Radicals in Thermally Activated Persulfate. *Industrial and Engineering Chemistry Research*, 48, 5558-5562.

Liu, H., Bruton, T. A., Doyle, F. M., Sedlak, D. L., 2014. *In situ* chemical oxidation of contaminated groundwater by persulfate: decomposition by Fe(III)- and Mn(IV)-containing oxides and aquifer materials. *Environmental Science & Technology*, 48, 10330-10336.

Liu, H., Bruton, T. A., Li, W., Van Buren, J., Prasse, C., Doyle, F. M., Sedlak, D. L., 2016. Oxidation of benzene by persulfate in the presence of Fe(III)- and Mn(IV)-containing oxides: stoichiometric efficiency and transformation products. *Environmental Science & Technology*, 50, 890-898.

Lu, J., Dong, W., Ji, Y., Kong, D., Huang, Q., 2016. Natural organic matter exposed to sulfate radicals increases its potential to form halogenated disinfection byproducts. *Environmental Science & Technology*. 50, 5060-5067.

Lutze, H. V., Kerlin, N., Schmidt, T. C., 2015. Sulfate radical-based water treatment in the presence of chloride: formation of chlorate, inter-conversion of sulfate radicals into hydroxyl radicals and influence of bicarbonate. *Water Research*, 72, 349-360.

Madhavan, V., Levanon, H., Neta, P., 1978. Decarboxylation by $SO_4^{\bullet-}$ radicals. *Radiation Research*, 15-22.

Mora, V. C., Rosso, J. A., Martire D. O., Gonzalez M. C., 2011. Phenol depletion by thermally activated peroxydisulfate at 70°C. *Chemosphere*, 84, 1270-1275.

Neta, P., Huie, R. E., Ross, A. B., 1988. Rate constants for reactions of inorganic radicals in aqueous solution. *Journal of Physical and Chemical Reference Data*. 17, 1027-1284.

Neta, P., Grodkowski, J., 2005. Rate constants for reactions of phenoxyl radicals in solutions. *Journal of Physical and Chemical Reference Data*. 34, 109-199.

Qian, Y., Guo, X., Zhang, Y., Peng, Y., Sun, P., Huang, C., Niu, J., Zhou, X., Crittiden, J. C., 2016. Perfluorooctanoic acid degradation using UV-persulfate process: modeling of the degradation and chlorate formation. *Environmental Science & Technology*, 50, 772-781.

Reynolds, D. A., 2014. United States Patent 9004816 B2.

Siegrist, R. L., Crimi, M., Simpkin, T. J., 2011. *In situ* chemical oxidation for groundwater remediation. Springer, NY.

Singh, U. C., Venkatarao, K., 1976. Decomposition of peroxodisulphate in aqueous alkaline solution. *Journal of Inorganic and Nuclear Chemistry*, 38, 541-543.

Sra, K. S., Thomson, N. R., Barker J. F., 2010. Persistence of persulfate in uncontaminated aquifer materials. *Environmental Science & Technology*, 44, 3098-3104.

Sun, P., Tyree, C., Huang, C.-H, 2016. Inactivation of E. coli, Bacteriophage MS2 and Bacillus Spores under d UV/H_2O_2 and UV/peroxydisulfate Advanced Disinfection Conditions. *Environmental Science & Technology*, 50(8), 4448-4458.

Tsitonaki, A., Petri, B., Crimi, M., Mosbæk, H., Siegrist, R. L., Bjerg, P. L., 2010. *In situ* chemical oxidation of contaminated soil and groundwater using persulfate: a review. *Critical Reviews in Environmental Science & Technology*, 40, 55-91.

Waldemer, R. H., Tratnyek, P. G., Johnson, R. O., Nurmi, J. T., 2007. Oxidation of chlorinated ethenes by heat-activated persulfate: kinetics and products. *Environmental Science & Technology*, 41, 1010-1015.

Yang, Y., Pignatello, J. J., Ma, J., Mitch, W. A., 2014. Comparison of halide impacts on the efficiency of contaminant degradation by sulfate and hydroxyl radical-based advanced oxidation processes (AOPs). *Environmental Science & Technology*, 48, 2344-2351.

Zafirou O.C., Voelker B., and Sedlak D.L., 1998. Chemistry of superoxide radical in seawater: reactions with inorganic Cu complexes. *Journal of Physical Chemistry* A. 102, 5693-5700.

Zazo, J. A., Casas, J. A., Mohedano, A. F., Gilarranz, M. A., Rodriguez, J. J., 2005. Chemical pathway and kinetics of phenol oxidation by Fenton's reagent. *Environmental Science & Technology*, 39, 9295-9302.

Zemei, H., Fessenden, R. W., 1978. The mechanism of reaction of $SO_4^{\bullet-}$ with some derivatives of benzoic acid. *The Journal of Physical Chemistry*, 82, 2670-2676.

Zhou, X. L., Mopper, K., 1990. Determination of photochemically produced hydroxyl radicals in seawater and freshwater. *Marine Chemistry*, 30, 71–88.

4.0 Mechanistic Study of Chlorendic Acid Removal by Heat-Activated Persulfate for ISCO Applications

4.1 Introduction

Chlorendic acid (CA) has been used historically for imparting flame retardancy to textiles and as an intermediate in the production of plasticizers (NTP, 1987). As a result, soil and groundwater contamination may be found at sites where the compound was manufactured or used. CA has also been found in landfill leachate at concentrations of several hundred mg/L possibly due to leaching from fire retarded products (Ying et al., 1986). It also exists in the environment as a degradation byproduct of certain pesticides, namely dieldrin, heptachlor and endosulfan (Cochrane and Forbes, 1974; Ali et al., 2016). CA is relatively hydrophilic (log K_{ow} = 1.86) and non-volatile under environmentally relevant conditions due to the negative charge associated with carboxyl groups (pKa 3.1). It can be removed by adsorption, but its solubility (K_{sp} = 0.7g/L), hydrophilicity, and charge suggest that the amount of adsorbent required would be prohibitively high. Apart from being resistant to biodegradation, the environmental fate of CA is not well understood (Sebastian et al., 1996). Few studies have investigated its mobility in the environment; however, compounds with a similar structure are persistent in the subsurface (Yang et al., 2005; Iwata et al., 1993). CA is considered toxic because it inhibits algal growth at around 0.6 mM (250 mg/L), is carcinogenic, and affects organ function in rats (Hendrix et al., 1983; NTP, 1987). The combination of toxicity and persistence have resulted in the ongoing consideration of chlorendic acid to be included in various toxic substances lists, though it is not yet listed in many cases since it does not bioaccumulate (ECHA, 2015).

More studies exploring the impact of CA on environmental and human health are required to be able to make decisive recommendations regarding this compound.

A literature search for investigations involving chlorendic acid revealed very few studies. Of these studies, a few show the destruction of CA by hydroxyl ($^{\bullet}OH$) and sulfate radicals ($SO_4^{\bullet-}$). For example, Stowell and Jensen found that ozone effectively dechlorinated CA by breaking the carbon-carbon double bond at a rate dependent on the production and scavenging of $^{\bullet}OH$ in solution, pH, dose, and the presence of bicarbonate (Stowell and Jensen, 1991). The same research group reported that CA is resistant to biological degradation (Sebastian et al., 1996). Hermes and Knupp demonstrated that electrochemically produced $^{\bullet}OH$ was successful in degrading CA. The authors suggest that ring cleavage results in the formation of short chain acids such as formic and acetic acid (Hermes and Knupp, 2015). Another group investigated the destruction of CA using gamma radiation and peroxymonosulfate (PMS). Their results show that $SO_4^{\bullet-}$ derived from PMS contributes to the destruction of CA even in the presence of radical scavengers such as carbonate, nitrite, and chloride (Shah et al., 2016). The authors provide second-order reaction rate constants of 1.75×10^9 $M^{-1}s^{-1}$ and 2.05×10^9 $M^{-1}s^{-1}$ for CA with $^{\bullet}OH$ and $SO_4^{\bullet-}$, respectively. The reported rate constants are surprising considering similar compounds, such as chlordane have rate constants with $^{\bullet}OH$ (6×10^8 $M^{-1}s^{-1}$), which are less than half of those described by Shah et al. (Haag and David Yao, 1992). Another investigation into the degradation of CA by $^{\bullet}OH$ produced photo-catalytically by UV/TiO_2 reported the production of HCl (via dehydrochlorination) and chlorendic anhydride (via dehydration) (Boisa, 2013). However, the detailed mechanism through which CA was

transformed was not described in all of these studies. Regardless of the reaction mechanism, it appears that $^{\bullet}OH$ and $SO_4^{\bullet-}$ are effective at degrading CA.

For radical-based processes to be employed to remediate sites contaminated with CA *in situ*, further research is needed to investigate the effect of factors such as pH, Cl^-, carbonate on the transformation of CA by $^{\bullet}OH$ and $SO_4^{\bullet-}$. The objectives of this study are to investigate the ability of heat- and mineral-activated $S_2O_8^{2-}$ to destroy CA. To gain insights into factors that can influence the rate of CA transformation, experiments were conducted employing solutions with different chemical compositions (*i.e.*, pH 4 – 8, $[HCO_3^-]$ = 0 – 10 mM, and $[Cl^-]$ = 0 – 5 mM.

4.2 Materials and Methods

4.2.1 Chemicals

All chemicals were of reagent grade and were used without further purification. Chlorendic acid, methyl tert-butyl ether (MTBE), and sodium persulfate were obtained from Sigma-Aldrich. Benzoic acid, potassium persulfate, potassium iodide, potassium phosphate, sodium sulfate, sodium chloride, sodium hydroxide, sulfuric acid and sodium bicarbonate were obtained from VWR International. All solutions were prepared using 18.2 MΩ·cm water (Millipore System).

4.2.2 Experimental setup

The degradation of CA by heat-activated $S_2O_8^{2-}$ was observed in homogenous solutions (*i.e.*, solid-free solutions) to systematically investigate the effect of pH as well as solutes such as HCO_3^- and Cl^- on the rate of CA transformation. The experiments were conducted in 16 mL sealed test tubes that contained 10 mL of reaction solution. The solution was

comprised of CA (50 - 100 µM), $S_2O_8^{2-}$ (1 mM), HCO_3^- (0 mM or 10 mM), chloride (0 mM or 5 mM), and benzoic acid (a model for competing contaminants, 10-100 µM). The solution pH was adjusted to pH 4 or 8 using 1 M H_2SO_4 or 1 M NaOH. The solution also contained 50 mM sodium sulfate, which served as background electrolyte to mitigate fluctuations in ionic strength caused by the production and consumption of ions.

Reactors were manually shaken daily and a water bath was used to control temperature to 40 or 70°C. In the case of room temperature experiments, reactors were placed on the bench. At predetermined time intervals, the activation of persulfate was quenched by submerging reactors in an ice bath, and the solution pH, oxidation-reduction potential (ORP), together with the concentrations of persulfate, chlorendic acid, chloride, chlorate, and total organic carbon (TOC) were measured. Experiments were performed in triplicate and average values along with one standard deviation are reported.

4.2.3 Analytical methods

Persulfate was measured spectrophotometrically using a modification of the Kolthoff potassium iodide method (Kolthoff and Belcher, 1957). TOC was measured on a Shimadzu organic carbon analyzer. Chlorendic acid was analyzed on a Thermo Scientific Ultimate 3000 ultra-high pressure liquid chromatograph equipped with a C_{18} column and a UV/vis photodiode array detector. In the case of the homogenous experiment, 1 mL samples were acidified with 50 µL of 1 M H_2SO_4 prior to HPLC analysis. In addition, 50 µL of methanol was added to each sample to quench any further oxidation reactions between CA and persulfate. The mobile phase consisted of 70% acetonitrile (ACN) and 30% 1 mM

H_2SO_4 at a flow rate of 0.8 mL/min. Chlorendic acid was detected with UV absorbance detection at 220 nm.

4.3 Results and Discussion

4.3.1 Reactivity of CA with $SO_4^{\bullet-}$ and $^{\bullet}OH$

As mentioned in the introduction section, a previous study reported that the reaction rates between CA and $^{\bullet}OH$ and $SO_4^{\bullet-}$ were 1.75×10^9 $M^{-1}s^{-1}$ and 2.05×10^9 $M^{-1}s^{-1}$, respectively. These values are somewhat high given that CA contains only one double bond but 6 chlorine atoms. Due to the chemical structure of CA, it is expected that CA would react with $^{\bullet}OH$ and $SO_4^{\bullet-}$ at slower rates. Therefore, the first step of this research was to re-measure the reaction rate constants to examine the reactivity of CA with $^{\bullet}OH$ and $SO_4^{\bullet-}$. The measurements were performed by Dr. Stephen Mezyk (Professor of Physical Chemistry, California State University at Long Beach), who is an expert in radical chemistry. Dr. Mezyk conducted a series of flash photolysis experiments, coupled with competitive kinetic studies, the results of which revealed that the reaction rates between CA and $^{\bullet}OH$ and $SO_4^{\bullet-}$ were $k_{OH} = 8.6 \times 10^7$ $M^{-1}s^{-1}$ and $k_{SO4} = 6.6 \times 10^7$ $M^{-1}s^{-1}$. These values were lower than the previously reported values, suggesting that background electrolytes that are more reactive with $^{\bullet}OH$ and $SO_4^{\bullet-}$ (*e.g.*, Cl^-) can greatly influence the rate of CA transformation.

4.3.2 Degradation of CA by Heat-Activated Persulfate

At 70°C, over seventy percent of the initial persulfate was consumed within six hours. Persulfate degradation was slightly enhanced in the presence of 10 μM benzoic acid (BA) and slightly delayed in the presence of 10 mM bicarbonate (HCO_3^-) (Figure 4.1). The

accelerated degradation in the presence of organic compounds has been observed in previous studies and is thought to be caused by radical chain reactions that propagate the decomposition of persulfate (Liang and Su, 2009; Liu et al., 2014). Many studies have reported the inhibitory effect of HCO_3^- on contaminant oxidation by activated persulfate, but few have mentioned the effect of HCO_3^- on persulfate activation rates (Huang et al., 2002; Liang et al., 2006; Waldemer et al., 2007).

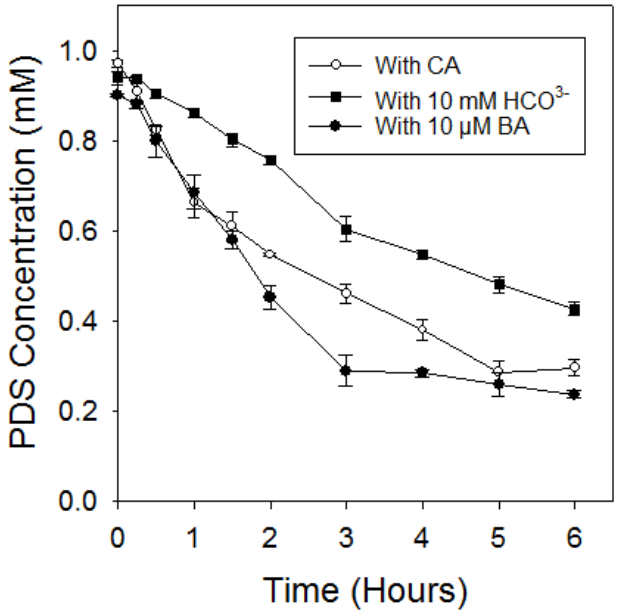

Figure 4.1: Thermal activation of persulfate (PDS). T = 70°C, $[S_2O_8^{2-}]_0$ = 1 mM, pH = 8.0 (buffered by 20 mM phosphate). Ionic strength was controlled with 50 mM Na_2SO_4

No CA degradation was observed in the absence of persulfate, suggesting that the loss of CA in the presence of persulfate was the result of oxidation (Figure 4.2A). At 70°C, all CA was removed from the solution within a few hours. CA concentration and TOC declined concurrently, suggesting that $SO_4^{\bullet-}$ is capable of mineralizing CA. Since 0.1 mM CA was fully degraded after 6 hours and each CA molecule contains 6 chlorine atoms, it was expected that 0.6 mM of chloride would be produced. The production of only 0.45 mM

chloride (Figure 4.2B) suggests that some chloride was still associated with the remaining organic compounds (approximately 10 mg/L TOC remained at the end of the experiment).

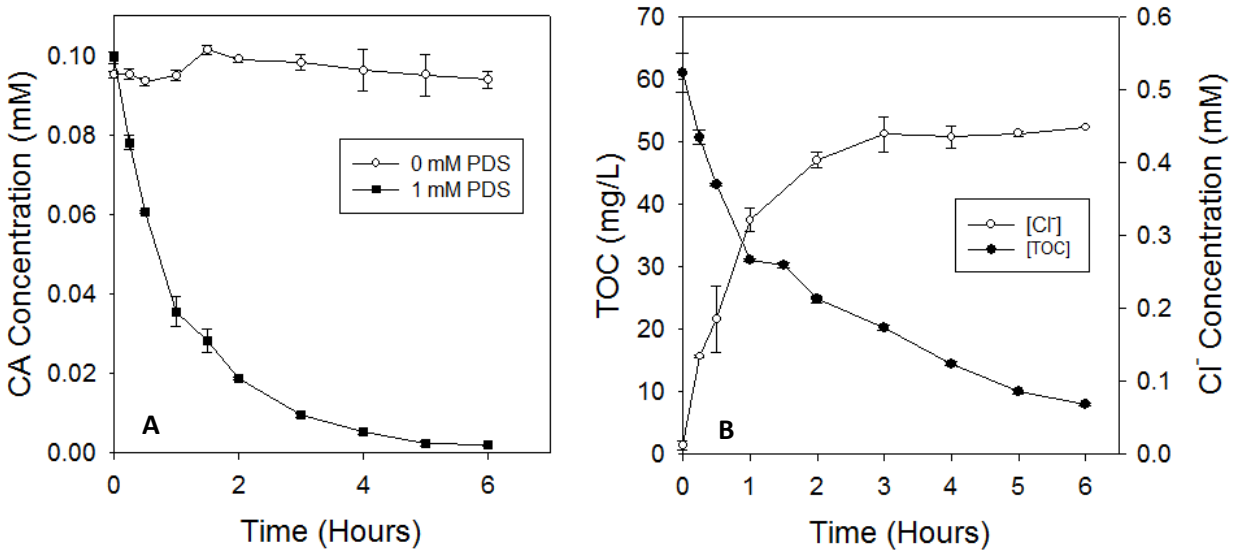

Figure 4.2: A. CA stability in the absence of persulfate and the destruction of CA by heat-activated persulfate (PDS) **B.** total organic carbon (TOC) and Cl^- production due to CA dechlorination T = 70°C, $[S_2O_8^{2-}]_0$ = 1 mM, $[CA]_0$ = 0.1 mM, pH = 8.0 (buffered by 20 mM phosphate), Ionic strength was controlled with 50 mM Na_2SO_4

4.3.3 Effect of Background Solutes on CA Degradation

In natural systems, the oxidation of contaminants is affected by groundwater constituents (*e.g.* chloride, bicarbonate) which decrease radical availability. To examine the effect of typical solutes, experiments were performed in the presence of bicarbonate, chloride, and a model competing contaminant (benzoic acid). The magnitude of the effect caused by these solutes is a function of their reaction rate constant with radical species (k) and solute concentration. Scavenging of $SO_4^{\bullet-}$ is also dependent on the predominant carbonate species which in turn depends on pH (reactions 4.10 - 4.14). Under environmentally relevant pH, bicarbonate (HCO_3^-) is the predominant carbonate species in solution (Stumm and Morgan, 1996). HCO_3^- has a relatively low reaction rate constant with $SO_4^{\bullet-}$ (reaction 4.13), but is present in the subsurface at concentrations which are

often several orders of magnitude above that of contaminants ([HCO_3^-] ≈ 1 - 30 mM). HCO_3^- is considered a scavenger because it reacts with $SO_4^{\bullet-}$ to produce the carbonate radical ($CO_3^{\bullet-}$) which is much less reactive than $SO_4^{\bullet-}$ and $^{\bullet}OH$. For example, the reaction rate constant for the oxidation of benzene by $CO_3^{\bullet-}$ is 10^6 times slower than that of $SO_4^{\bullet-}$ and benzene (Chen et al., 1975; Neta et al., 1977). The reactions listed below summarize the relevant species of carbonate and their interactions with the sulfate radical.

$$HCO_3^- \leftrightarrow H^+ + CO_3^{2-} \qquad \text{pKa = 10.3} \qquad (4.10)$$

$$H_2CO_3 \leftrightarrow H^+ + HCO_3^- \qquad \text{pKa = 6.4} \qquad (4.11)$$

$$SO_4^{\bullet-} + H_2CO_3 \rightarrow SO_4^{2-} + CO_3^{\bullet-} \qquad (4.12)$$

$$SO_4^{\bullet-} + HCO_3^- \rightarrow SO_4^{2-} + CO_3^{\bullet-} \qquad (4.13)$$

$$SO_4^{\bullet-} + CO_3^{2-} \rightarrow SO_4^{2-} + CO_3^{\bullet-} \qquad (4.14)$$

In our system, the presence of HCO_3^- significantly constrained the ability of activated persulfate to oxidize CA (Figure 4.3). With 10 mM HCO_3^- in solution, 1 mM $S_2O_8^{2-}$ activated at 70°C only degraded 22% of CA after 6 hours in comparison to 99% degradation in the absence of HCO_3^-. As previously mentioned, the presence of HCO_3^- is known to have inhibitory effects on contaminant oxidation by activated persulfate (Huang et al., 2002; Liang et al., 2006; Waldemer et al., 2007). Competition occurs below pH 10.3 due to the reaction between HCO_3^- and $SO_4^{\bullet-}$, resulting in formation of the relatively weak carbonate radical $CO_3^{\bullet-}$ (Huie et al., 1991) (reaction 4.13). Environmental systems which contain elevated concentrations of HCO_3^- will require higher doses of amendment than those with lower concentrations in order to effectively degrade CA.

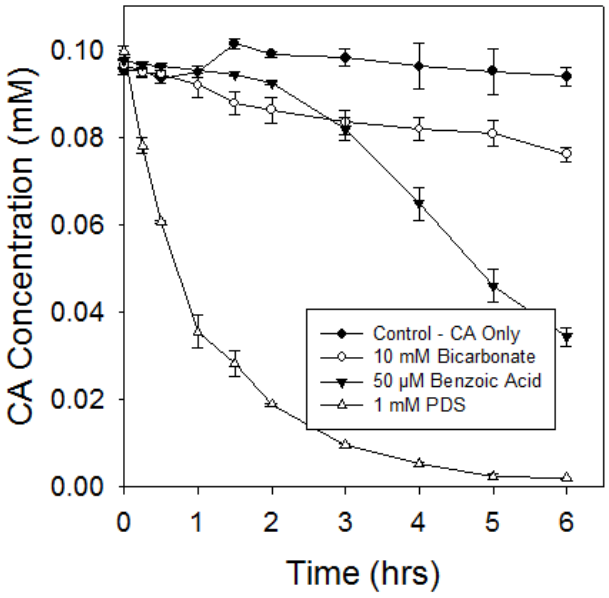

Figure 4.3: CA Degradation by heat-activated persulfate (PDS) in the presence of bicarbonate and benzoic acid. T = 70°C, $[S_2O_8^{2-}]_0$ = 1 mM, $[CA]_0$ = 0.1 mM, pH = 8.0 (buffered by 20 mM phosphate), Ionic strength was controlled with 50 mM Na_2SO_4

Chloride (Cl^-) is also ubiquitous in environmental systems and has been known to suppress the degradation of contaminants in some cases, and accelerate degradation in others (Bennedson et al., 2012; Liang et al., 2006). Chloride is important because it is quite reactive with $SO_4^{\bullet-}$, with $k_{SO4\bullet-}$ = 2.6 x 10^8 $M^{-1}s^{-1}$ (Padmaja et al., 1993), and is a common co-contaminant to chlorinated pollutants. To investigate the effect of chloride on CA degradation by heat-activated persulfate degradation rates were observed and compared at 0 and 5 mM Cl^-. When compared to experiments without chloride, the presence of 5 mM Cl^- accelerated CA degradation at pH 4 and impedes degradation at pH 8 (Figure 4.4).

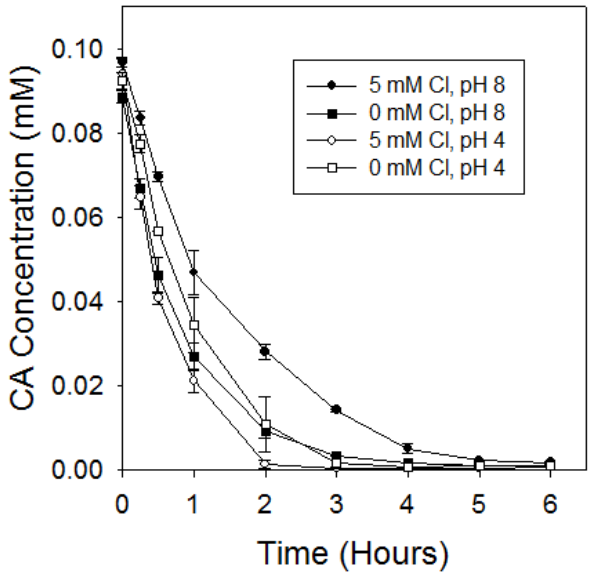

Figure 4.4: CA degradation in the absence and presence of chloride (5 mM) at pH 4 and 8. T = 70°C, $[S_2O_8^{2-}]_0$ = 1 mM, $[CA]_0$ = 0.1 mM, pH buffered by 20 mM phosphate, Ionic strength was controlled with 50 mM Na_2SO_4

Accelerated degradation at pH 4 is unexpected because previous studies have observed that below pH 5 $SO_4^{\bullet-}$ is scavenged by chloride to form chlorate (ClO_3^-) according to the following reaction scheme (Lutze et al., 2015):

$SO_4^{\bullet-} + Cl^- \rightarrow SO_4^{2-} + Cl^{\bullet}$	(Padmaja et al., 1993)	(4.15)
$Cl^{\bullet} + H_2O \rightarrow HOCl^{\bullet-} + H^+$	(Buxton et al., 1998)	(4.16)
$HOCl^{\bullet-} + H_2O \rightarrow OH^{\bullet} + Cl^-$	(Jayson et al., 1973)	(4.17)
$Cl^{\bullet} + Cl^- \leftrightarrow Cl_2^{\bullet-}$	(Nagarajan and Fessenden, 1985)	(4.18)
$Cl_2^{\bullet-} + Cl_2^{\bullet-} \rightarrow Cl_2 + 2Cl^-$	(Yu et al., 2004)	(4.19)
$Cl_2 + H_2O \rightarrow HOCl + Cl^- + H^+$	(Lifshitz and Perlmutter-Hayman, 1960)	(4.20)
$HOCl \leftrightarrow H^+ + ClO^-$	(Haag and Hoigne, 1983)	(4.21)
$ClO^- + OH^{\bullet} \rightarrow ClO^{\bullet} + OH^-$	(Buxton and Subhani, 1972)	(4.22)
$2ClO^{\bullet} + H_2O \rightarrow ClO^- + ClO_2^- + 2H^+$	(Kläning and Wolff, 1985)	(4.23)
$ClO_2^- + OH^{\bullet} \rightarrow ClO_2^{\bullet} + OH^-$	(Kläning et al., 1985)	(4.24)

$$ClO_2^{\bullet} + OH^{\bullet} \rightarrow ClO_3^{-} + H^{+}$$ (Kläning et al., 1985) (4.25)

50 µM chlorate (data not shown) was produced at pH 4 with 5 mM chloride, but this apparently did not negatively impact the CA degradation rate. This inconsistency could be explained by the effect of temperature on each reaction rate constant according to Arrhenius' equation:

$$k = Ae^{-\frac{Ea}{RT}}$$

Neither the frequency factor (A), nor the activation energy (Ea) for any reactions involving chlorendic acid are available. It is possible that temperature disproportionately increases the reaction rate constant for the reaction between $SO_4^{\bullet-}$ and CA (Reaction 4.26) relative to reaction 4.15 in the chlorate production scheme.

$$SO_4^{\bullet-} + CA \rightarrow Products$$ (4.26)

pH alone had no significant effect on CA degradation between pH 4 and 8 (Figure 4.4). This is consistent with the observation that $SO_4^{\bullet-}$ is the predominant reactive species below pH 9 in the absence of chloride (Fang et al., 2012). Additionally, there was no change in CA degradation rate observed due to hydrolysis at pH 8, and chloride had no effect on the activation kinetics of persulfate activation (data not shown).

In the subsurface, other contaminants may act as radical scavengers reducing oxidation efficiency between activated persulfate and chlorendic acid. Benzoic acid (BA) was used as a model compound to represent a competing contaminant. When BA is present in solution with activated persulfate and chlorendic acid it is quickly oxidized, causing a dose-dependent lag period before CA begins to degrade (Figure 4.5). This was expected

due to the disparity in reaction rate constants and concentrations of CA and BA. The reaction rate constant between BA and $SO_4^{\bullet-}$ is 1.2 x 10^9 $M^{-1}s^{-1}$ (Neta et al. 1988), nearly twenty-fold the measured reaction rate constant for $SO_4^{\bullet-}$ and CA at 25°C of 6.6 x 10^7 $M^{-1}s^{-1}$ (reported in section 4.1.1). Since CA is less reactive with $SO_4^{\bullet-}$ relative to many common contaminants, the presence of any co-contaminants will likely inhibit or delay oxidation of CA. Competing contaminant oxidant demand can be overcome by providing sufficient oxidant dose.

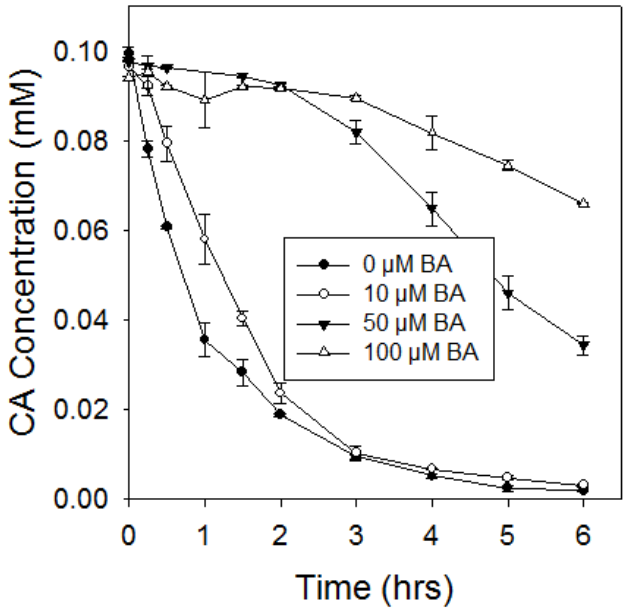

Figure 4.5: CA oxidation by heat-activated persulfate with dose-dependent radical scavenging by benzoic acid (BA). T = 70°C, $[S_2O_8^{2-}]_0$ = 1 mM, $[CA]_0$ = 0.1 mM, pH = 8.0 (buffered by 20 mM phosphate), Ionic strength was controlled with 50 mM Na_2SO_4

4.4 Conclusion

This study examined the effect of temperature, pH and background solute on chlorendic acid degradation rate. Conclusions are summarized as follows:

- The reaction rate constant between two radical species ($^{\bullet}OH$ and $SO_4^{\bullet-}$) and CA were measured (by Dr. Stephen Mezyk) as 8.6 x 10^7 $M^{-1}s^{-1}$ and 6.6 x 10^7 $M^{-1}s^{-1}$

respectively. These measurements suggest CA is less reactive than many other common contaminants.

- CA was completely degraded by heat-activated persulfate at 70°C within 6 hours. Synchronous decrease in TOC and formation of chloride suggest that CA is being oxidized. Since previous studies suggest that $SO_4^{\bullet-}$ is the predominant radical species under our experimental conditions, it is concluded that $SO_4^{\bullet-}$ is capable of mineralizing CA.

- Background solutes were found to impact the activation of persulfate and the degradation of CA. 5 mM chloride was observed to accelerate CA degradation at pH 4 but impede degradation at pH 8. Neither chloride, nor pH alone had a significant effect on CA degradation rate. HCO_3^- both slowed persulfate activation as well as CA degradation. This supports the well documented hypothesis wherein HCO_3^- reacts with $SO_4^{\bullet-}$ to produce the weakly reactive carbonate radical. When benzoic acid was present in solution with CA and heat-activated persulfate, $SO_4^{\bullet-}$ preferentially reacted with BA. When designing ISCO systems for the remediation of sites contaminated with CA, the presence (and formation) of background solutes must be carefully considered in order to avoid ineffective treatment.

4.5 References

Ali, M., K. M. Gani, A. A. Kazmi, and N. Ahmed. "Degradation of Aldrin and Endosulfan in Rotary Drum and Windrow Composting." *Journal of Environmental Science and Health, Part B* 51.5 (2016): 278-86.

Bennedsen, L. R., J. Muff, and E. G. Søgaard. "Influence of Chloride and Carbonates on the Reactivity of Activated Persulfate." *Chemosphere* 86.11 (2012): 1092-097.

Boisa, N. "Photo-catalytic Degradation of Chlorendic Acid: 1. Degradation Products." *Journal of Applied Sciences and Environmental Management* 17.3 (2013).

Buxton, G. V., and M. S. Subhani. "Radiation Chemistry and Photochemistry of Oxychlorine Ions. Part 2.—Photodecomposition of Aqueous Solutions of Hypochlorite Ions." *Journal of the Chemical Society, Faraday Transactions 1: Physical Chemistry in Condensed Phases* 68.0 (1972): 958.

Buxton, G. V., M. Bydder, and G. Arthur Salmon. "Reactivity of Chlorine Atoms in Aqueous Solution: Part 1 The Equilibrium $Cl^{\bullet} + Cl^{-} <-> Cl_2^{\bullet-}$." *Journal of the Chemical Society, Faraday Transactions* 94.5 (1998): 653-57.

Chen, S., M. Z. Hoffman, and G. H. Parsons. "Reactivity of the Carbonate Radical toward Aromatic Compounds in Aqueous Solution." *The Journal of Physical Chemistry* 79.18 (1975): 1911-912.

Cochrane, W. P., and M. A. Forbes. "Oxidation Products of Heptachlor and its Metabolites." *Chemosphere* 3.1 (1974): 41-46.

European Chemicals Agency (ECHA), PACT – RMOA and hazard assessment activities. website. echa.europa.eu. Updated April 2015. Accessed April 2017.

Fang, G., D. D. Dionysiou, Y. Wang, S. R. Al-Abed, and D. Zhou. "Sulfate Radical-based Degradation of Polychlorinated Biphenyls: Effects of Chloride Ion and Reaction Kinetics." *Journal of Hazardous Materials* 227-228 (2012): 394-401.

Haag, W. R., and J. Hoigné. "Ozonation of Water Containing Chlorine or Chloramines. Reaction Products and Kinetics." *Water Research* 17.10 (1983): 1397-402.

Haag, W. R., and C. C. David Yao. "Rate Constants for Reaction of Hydroxyl Radicals with Several Drinking Water Contaminants." *Environmental Science & Technology* 26.5 (1992): 1005-013.

Hendrix, P. F., J. A. Hamala, C. L. Langner, and H. P. Kollig. "Effects of Chlorendic Acid, a Priority Toxic Substance, on Laboratory Aquatic Ecosystems." *Chemosphere* 12.7-8 (1983): 1083-099.

Hermes, N., and G. Knupp. "Transformation of Atrazine, Bisphenol A and Chlorendic Acid by Electrochemically Produced Oxidants Using a Lead Dioxide Electrode." *Environmental Science: Water Research & Technology* 1.6 (2015): 905-12.

Huang, K., R. A. Couttenye, and G. E. Hoag. "Kinetics of Heat-assisted Persulfate Oxidation of Methyl Tert-butyl Ether (MTBE)." *Chemosphere* 49.4 (2002): 413-20.

Huie, R.E., C. L. Clifton, and P. Neta. "Electron Transfer Reaction Rates and Equilibria of the Carbonate and Sulfate Radical Ions." *Radiation Physics and Chemistry* 38.5 (1991): 477-81.

Iwata, H., S. Tanabe, N. Sakai, A. Nishimura, and R. Tatsukawa. "Geographical Distribution of Persistent Organochlorines in Air, Water and Sediments from Asia and Oceania, and Their Implications for Global Redistribution from Lower Latitudes." *Environmental Pollution* 85.1 (1994): 15-33.

Jayson, G. G., B. J. Parsons, and A. J. Swallow. "Some Simple, Highly Reactive, Inorganic Chlorine Derivatives in Aqueous Solution. Their Formation Using Pulses of Radiation and Their Role in the Mechanism of the Fricke Dosimeter." *Journal of the Chemical Society, Faraday Transactions 1: Physical Chemistry in Condensed Phases* 69.0 (1973): 1597.

Johnson, R. L., P. G. Tratnyek, and Reid O'Brien Johnson. "Persulfate Persistence under Thermal Activation Conditions." *Environmental Science & Technology* 42.24 (2008): 9350-356.

Kläning, U. K., K. Sehested, and J. Holcman. "Standard Gibbs Energy of Formation of the Hydroxyl Radical in Aqueous Solution. Rate Constants for the Reaction $ClO^{2-} + O_3 <-> O_3^- + ClO_2$" *The Journal of Physical Chemistry* 89.5 (1985): 760-63.

Kläning, U. K., and T. Wolff. "Laser Flash Photolysis of HClO, ClO^-, HBrO, and BrO^- in Aqueous Solution. Reactions of Cl- and Br-Atoms." *Berichte Der Bunsengesellschaft Für Physikalische Chemie* 89.3 (1985): 243-45.

Kolthoff, I.M, and R. Belcher. *Titration Methods Oxidation-reduction Reactions*. New York: Interscience, 1957.

Liang, C., Z. Wang, and N. Mohanty. "Influences of Carbonate and Chloride Ions on Persulfate Oxidation of Trichloroethylene at 20 °C." *Science of the Total Environment* 370.2-3 (2006): 271-77.

Lifshitz, A., and B. Perlmutter-Hayman. "The Kinetics of the Hydrolysis of Chlorine. I. Reinvestigation of the Hydrolysis in Pure Water." *The Journal of Physical Chemistry* 64.11 (1960): 1663-665.

Lutze, H. V., N. Kerlin, and T. C. Schmidt. "Sulfate Radical-based Water Treatment in Presence of Chloride: Formation of Chlorate, Inter-conversion of Sulfate Radicals into Hydroxyl Radicals and Influence of Bicarbonate." *Water Research* 72 (2015): 349-60.

NTP Technical Report on the Toxicology and Carcinogenesis Studies of Chlorendic Acid (CAS No. 115-28-6) in F344/N Rats and B6C3F₁ Mice (feed Studies). Research Triangle Park, NC: National Toxicology Program, U.S. Dept. of Health and Human Services, Public Health Service, National Institutes of Health, 1987.

Nagarajan, V., and R. W. Fessenden. "Flash Photolysis of Transient Radicals. 1. X_2^- with X = Cl, Br, I, and SCN." *The Journal of Physical Chemistry* 89.11 (1985): 2330-335.

Neta, P., Huie, R. E., Ross, A. B., 1988. “Rate constants for reactions of inorganic radicals in aqueous solution.” *Journal of Physical and Chemical Reference Data*. 17, 1027-1284.

Neta, P., V. Madhavan, H. Zemel, and R. W. Fessenden. "Rate Constants and Mechanism of Reaction of Sulfate Radical Anion with Aromatic Compounds." *Journal of the American Chemical Society* 99.1 (1977): 163-64.

Padmaja, S., P. Neta, and R. E. Huie. "Rate Constants for Some Reactions of Inorganic Radicals with Inorganic Ions. Temperature and Solvent Dependence." *International Journal of Chemical Kinetics* 25.6 (1993): 445-55.

Sebastian, J. H., A. S. Weber, and J. N. Jensen. "Sequential Chemical/biological Oxidation of Chlorendic Acid." *Water Research* 30.8 (1996): 1833-843.

Shah, N. S., J. A. Khan, Ala’A H. Al-Muhtaseb, M. Sayed, B. Murtaza, and Hasan M. Khan. "Synergistic Effects of HSO_5^- in the Gamma Radiation Driven Process for the Removal of Chlorendic Acid: A New Alternative for Water Treatment." *Chemical Engineering Journal* 306 (2016): 512-21.

Stowell, J. P., and J. N. Jensen. "Dechlorination of Chlorendic Acid with Ozone." *Water Research* 25.1 (1991): 83-90.

Stumm, W., and J. J. Morgan. *Aquatic Chemistry: Chemical Equilibria and Rates in Natural Waters*. New York: Wiley, 1996.

Waldemer, R. H., P. G. Tratnyek, R. L. Johnson, and J. T. Nurmi. "Oxidation of Chlorinated Ethenes by Heat-Activated Persulfate: Kinetics and Products." *Environmental Science & Technology* 41.3 (2007): 1010-015.

Yang, R., G. Jiang, Q. Zhou, C. Yuan, and J. Shi. "Occurrence and Distribution of Organochlorine Pesticides (HCH and DDT) in Sediments Collected from East China Sea." *Environment International* 31.6 (2005): 799-804.

Ying, W., J. J. Duffy, and M. E. Tucker. "Removal of Humic Acid and Toxic Organic Compounds by Iron Precipitation." *Environmental Progress* 7.4 (1988): 262-69.

Ying, W., R.R. Bonk, V.J. Lloyd, and S.A. Sojka. "Biological Treatment of a Landfill Leachate in Sequencing Batch Reactors." *Environmental Progress* 7.4 (1986): 41-50.

Yu, X., Z. Bao, and J. R. Barker. "Free Radical Reactions Involving $Cl^{\bullet}$, and $Cl_2^{-\bullet}$, and $SO_4^{-\bullet}$ in the 248 nm Photolysis of Aqueous Solutions Containing $S_2O_8^{2-}$ and Cl^-." *ChemInform* 35.14 (2004).

5.0 Conclusions and Recommendations

Persulfate is currently being used for *in situ* remediation of contaminants. When persulfate is activated by heat, metals, base, or others, radical species ($SO_4^{\bullet-}$ and $^{\bullet}OH$) are formed which are powerful oxidants. With its diverse activation options, lifetime in the subsurface, high oxidation efficiency, and the opportunity for mobilization using electrokinetics, persulfate has proven to be very useful for remediation. This study examined the effects of environmental factors that may affect the kinetics and transformation mechanisms of contaminant oxidation by activated persulfate.

For benzoic acid (BA), temperature played a significant role in the branching of transformation mechanisms. At higher temperatures, decarboxylation byproducts (phenol, catechol, hydroquinone) were the predominant species, while at lower temperatures there were more hydroxylation byproducts (2-, 3-, 4-hydroxybenzoic acid). Temperature did not affect oxidation efficiency ($E = \Delta[BA]/ \Delta[S_2O_8^{2-}]$) x 100%, though BA concentration did; at room temperature, E slightly decrease as [BA] increased from 0.5 to 2 mM, while at 70°C the opposite is true.

Future work should examine the impact of temperature on the oxidation efficiency and transformation mechanisms of other contaminants. Additionally, transformation mechanisms and byproduct distribution should be considered when other experimental parameters, such as pH, are varied.

Results from experiments involving chlorendic acid (CA) indicate that the sulfate radical is capable of completely removing (with some mineralization) 0.1 mM CA at 40°C within

6 hours. pH did not affect degradation rate until chloride was introduced; degradation was accelerated at pH 4 and reduced at pH 8 in the presence of 5 mM chloride. Bicarbonate and benzoic acid (representing a competing contaminant) inhibited CA degradation by heat-activated persulfate. Future work regarding chlorendic acid should focus on oxidation byproduct identification, and optimizing oxidant dose and efficiency.